ioMosaic®

Minimizing risk. Maximizing potential.®

Quantify Explosion Venting Dynamics in Vessels, Enclosures, and Energy Storage Systems

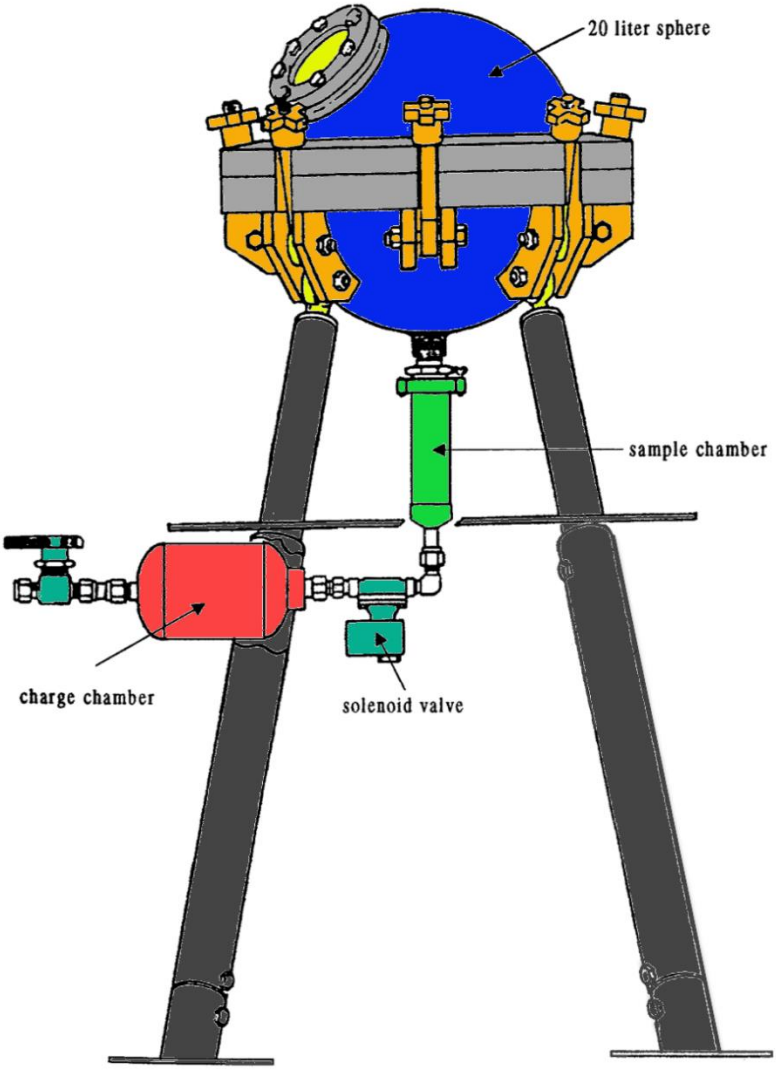

An ioMosaic Corporation White Paper

G. A. Melhem, Ph.D., FAIChE

melhem@iomosaic.com

IOMOSAIC CORPORATION

Quantify Explosion Venting Dynamics in Vessels, Enclosures, and Energy Storage Systems

Process Safety and Risk Management Practices

authored by

Georges A. MELHEM, Ph.D., FAIChE

April 6, 2022

Contents

1 Introduction

Explosions can occur in vessels or enclosures containing flammable gases and/or dusts. Explosion venting, often referred to as deflagration venting (because we cannot practically vent detonations), is used to protect from catastrophic vessel/enclosure failure. Simplified equations are often used to determine the deflagration relief requirements. Simplified equations can be found in standards such as NFPA 68 [1]. While easy to use, simplified equations tend to overestimate the relief requirements and have several practical limitations.

Simplified equations provided in NFPA 68 [1] require the use of an explosion severity index, usually obtained from actual testing in a 20 liter sphere or a 1 m^3 vessel. Published severity index data for flammable gases or dusts are also used. Typically, simplified equations for deflagration venting apply to ideal geometries and for short vent lines. They are not readily applicable to complex geometries, systems with elevated initial temperatures or pressures, hybrid systems containing flammable gases and dusts, systems with diluents and/or chemical oxidizers, systems with reduced venting set pressures, geometries with long L/D ratios or geometries with long vent piping where flame acceleration becomes significant.

We have developed detailed deflagration and explosion dynamics methods and computer codes that address many of the shortcomings of simplified sizing methods. These dynamic methods rely on a detailed representation of all possible independent combustion reaction(s) using direct Gibbs free energy minimization [2, 3, 4] coupled with a detailed burning rate model developed from measured explosion data using a 20 liter sphere or a 1 m^3 vessel. We describe these methods in what follows and provide examples of how they are applied and how the burning rate models are developed from measured data.

2 What is An Explosion Severity Index ?

Explosions in closed and vented enclosures and/or vessels have been studied extensively in the literature for combustible gases and dusts. Most of the published data deals with central ignition in spherical vessels of varying size. It has been shown for many hydrocarbon fuel-air and dust-air explosions in spherical vessels or enclosures with low length to diameter ratio ($\frac{L}{D} \simeq 1$), that the maximum explosion pressure rise rate is related to the enclosure volume by the following equation:

$$V^{1/3}\left[\frac{dP}{dt}\right]_{\max} = \text{constant} = K, \quad \text{or} \tag{1}$$

$$\left[\frac{dP}{dt}\right]_{\max} = \frac{K}{V^{1/3}} \tag{2}$$

$$\tag{3}$$

V is the vessel volume in m^3 and K is defined as the explosion severity index in $(\mathrm{bar.m/s})$ and is normally a measured property (see Figure 1). The explosion severity index for a gas is referred to as K_g while for dusts it is referred to as K_{st}. The subscript st is an abbreviation for the German word for dust, staub.

Tables 1 and 2 show typical values for K_{st} and K_g for various dusts and gases. It is important to note that these values are functions of composition, particle size, moisture content, turbulence

Figure 1: A typical pressure-time profile measured using the 20 liter dust sphere

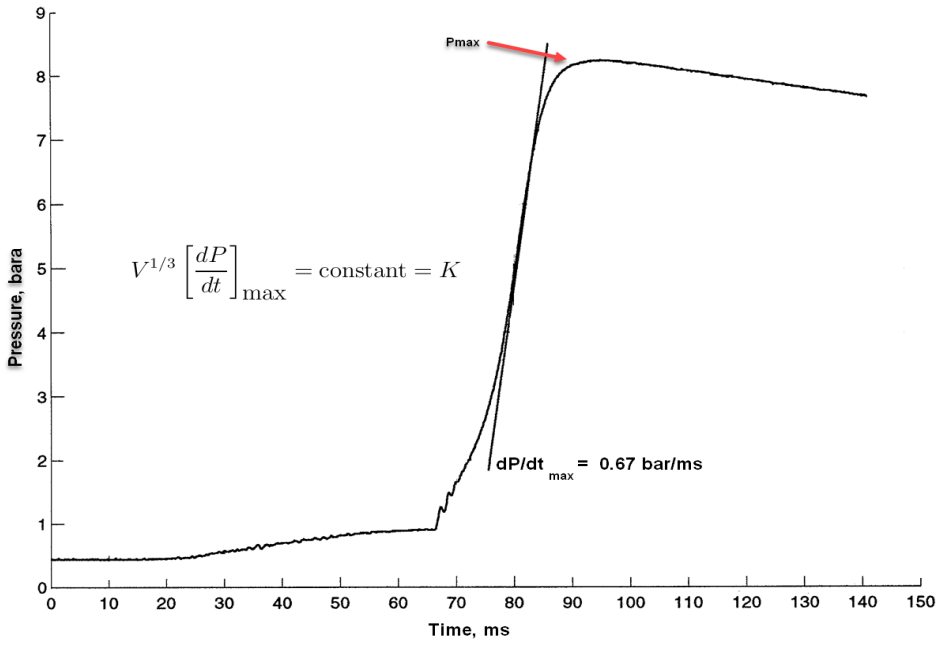

generation and mixing within the test vessel, and the ignition source energy and duration. The explosion severity index K and maximum non-vented vessel pressure $P_{\max}$ depend linearly on initial pressure. Higher values of initial pressure will result in higher values of K and $P_{\max}$.

3 How do We Measure the Explosion Severity Index?

The value of K is determined experimentally in an explosion apparatus for vapors or dusts (see Figure 1). The apparatus is a spherical vessel with a centrally located igniter. For gases, the vessel is evacuated first. Then the gas is metered into the vessel to obtain the required concentration. Ignition is initiated using a spark and pressure is then measured as a function of time.

The procedure for dusts employs a vessel with a sample holder and a distribution ring to insure proper mixing prior to ignition. The dust is delivered to the sphere using air pressure which drives the dust from the sample holder through the distribution ring into the vessel. The vessel pressure prior to ignition is normally one atmosphere. Ignition is induced via a spark after allowing sufficient time for mixing (typically on the order of milliseconds).

Measured values may not directly scale up to vessels larger then 20 m^3 in volume or vessels with large L/D ratios [1]. For enclosures with large L/D ratios or large blockage ratios (obstacles) flame acceleration becomes important. Resulting damage can be different from what is exhibited in low L/D explosions and tends to be localized and very severe. Flame acceleration can lead to a deflagration to detonation transition (DDT).

Table 1: K_{st} values of technical fine dusts (high ignition energy) [5]

Dust	P_{max} (bar)	K_{st} (bar-m/s)
PVC	6.7 - 8.5	27 - 98
Milk Powder	8.1 - 9.7	58 - 130
Polyethylene	7.4 - 8.8	54 - 131
Sugar	8.2 - 9.4	59 - 131
Resin dust	7.8 - 8.9	108 - 174
Brown coal	8.1 - 10.0	93 - 176
Wood dust	7.7 - 10.5	83 - 211
Cellulose	8.0 - 9.8	56 - 229
Pigments	6.5 - 10.7	28 - 344
Aluminum	5.4 - 12.9	16 - 750

Table 2: Average K_g values for gases ignited at zero turbulence [5]

Gas	K_g (bar-m/s)
Methane	55
Propane	75
Hydrogen	550

4 How Do We Correlate Explosion Severity with Burning Rate?

The explosion severity index is directly related to the combustion reactions rates or the burning velocity, s_f. Bradley and Mitcheson [6, 7] used a simplified adiabatic deflagration model to illustrate to dependence of K on a constant burning velocity:

$$K = \left[\frac{dP}{dt}\right]_{\max} V^{1/3} = (36\pi)^{1/3} (P_{max} - P_0) \left(\frac{P_{max}}{P_0}\right)^{1/\gamma_u} s_f \tag{4}$$

where P_{max} is the measured or calculated constant volume pressure in bara, P_0 is the starting pressure in bara, γ_u is the unburnt gas (or dust/air mixture) heat capacity ratio, and s_f is the burning velocity in $\mathrm{m/s}$. Equation 4 can be rearranged to estimate s_f from measured or reported explosion severity index data:

$$s_f = \left(\frac{V}{36\pi}\right)^{1/3} \left(\frac{P_0}{P_{max}}\right)^{1/\gamma_u} \left(\frac{1}{P_{max} - P_0}\right) \left[\frac{dP}{dt}\right]_{\max} \tag{5}$$

For a spherical vessel with a radius r (in m), s_f becomes:

$$s_f = \left(\frac{r}{27}\right)\left(\frac{P_0}{P_{max}}\right)^{1/\gamma_u}\left(\frac{1}{P_{max}-P_0}\right)\left[\frac{dP}{dt}\right]_{\max} \quad (6)$$

The data shown in Figure 1 implies a flame speed of $1.09\ \mathrm{m/s}$ assuming a heat capacity ratio of 1.4:

$$s_f = \left(\frac{20\times10^{-3}}{36\pi}\right)^{1/3}\left(\frac{1}{8.5}\right)^{1/1.4}\left(\frac{1}{8.5-1}\right)[670] \quad (7)$$

$$= 5.61\times10^{-2}\times0.216\times0.133\times670 = 1.09\ \mathrm{m/s} \quad (8)$$

Similarly, K can be calculated using Equation 4 if measured or published values of the laminar burning velocity and maximum constant volume pressure are provided. Ogle [8] provides a simple expression for the estimation of dust clouds burning velocity based on constant pressure adiabatic flame temperature and the the assumption that flame propagation heat transfer occurs predominantly by radiation:

$$s_f \simeq \frac{\sigma T_f^4}{\rho_{m,0}c_{p,m}\left(T_f-T_u\right)} \quad (9)$$

where σ is Boltzman's constant which is equal to $5.67\times10^{-8}\ \mathrm{W/m^2/K^4}$, T_f is adiabatic flame temperature in K, $\rho_{m,0}$ is the starting initial dust/air mixture density in $\mathrm{kg/m^3}$, $c_{p,m}$ is the mixture specific heat in $\mathrm{J/kg/K}$, and T_u is the unburnt dust/air mixture temperature in K.

Equation 5 can also be used to approximate the the burning velocity of a material where K is measured referenced to a similar material with known K and s_f values:

$$s_{f_2} = s_{f_1}\left[\frac{K_2}{K_1}\right]\left[\frac{P_{max_1}-P_0}{P_{max_2}-P_0}\right]\left[\frac{\left(\frac{P_{max_1}}{P_0}\right)^{1/\gamma_{u_1}}}{\left(\frac{P_{max_2}}{P_0}\right)^{1/\gamma_{u_2}}}\right] \quad (10)$$

$$\simeq s_{f_1}\left[\frac{K_2}{K_1}\right] \quad (11)$$

5 Explosion Severity Index Testing Apparatus

K_g is often measured using a 5 liter steel sphere rated for high pressure [1]. The sphere is placed within an oven enclosure. A hastelloy sphere can be used when the gases being tested are corrosive to steel. Ignition is achieved using an arc ignition source. Data acquisition is similar to what is used in a 20 liter sphere. A high speed data acquisition system records the pressure as a function of time.

K_{st} values are typically measured using a 20 liter sphere (See Figure 2). The 20 liter sphere can be used to obtain useful information on the deflagration characteristics of dust clouds for explosion

[1] see BS EN 15967-2011 for typical requirements

venting, inerting, or suppression design. This includes determination of the lower explosive limit (LEL), upper explosive limit (UEL), limiting oxygen concentration (LOC), maximum pressure (P_{max}), rate of maximum pressure rise, and K_{st} value. A 1 m^3 vessel has also been used but requires a much larger dust sample.

A typical deflagration pressure profile from a 20 liter sphere is shown in Figure 1. The 20 liter test sphere is typically operated as follows:

1. The test substance is loaded in the sample holder.
2. The sphere is partially evacuated and the charge chamber is pressurized to 300 psig with air.
3. A timing circuit is activated which opens the charge chamber solenoid. The air from the charge chamber carries the dust sample into the sphere passing through a dispersing nozzle.
4. After a prescribed time delay a pyrotechnic igniter (10 kJ) ignites the dust cloud. Two 5 kJ igniters can also be used. The energy release from a 10 kJ igniter produces a pressure increase in the range of 0.6 to 0.8 bara in the 20 liter sphere. This value is typically subtracted from the maximum measured pressure when the data is reported.

A high speed data acquisition system records the pressure as a function of time. The concentration is varied to achieve the maximum pressure and rate of pressure rise. Concentrations can be varied to determine the LEL and UEL. The LOC can be determined by varying the oxygen concentration in the charge chamber and partially evacuated sphere to the point where deflagrations do not occur.

Measured characteristics of the dust will depend on particle size, particle distribution and moisture content. The measured rate of pressure rise depends on levels of turbulence and the energy of the ignition source which may not necessarily be reflected in the plant environment to which the results are being applied.

6 Anatomy of Deflagration Venting Dynamics

Adequate explosion venting requires a volumetric relief rate that equals or exceeds the volumetric generation rate due to chemical combustion and/or decomposition in a given enclosure. For enclosures with open vents and depending on the ignition location relative to the vent, unburnt reactants may be first vented followed by a mixture of combustion products and reactants when the flame reaches the vicinity of the vent. For enclosures with initially closed vents, vent opening dynamics become important. Turbulence generation following vent opening can lead to flame acceleration which then causes higher overpressure in the enclosure than what the vent may be designed for. This is illustrated in Figure 3.

During a deflagration, pressure rise is a function of time (see Figure 1) and the burning velocity increases with time because of adiabatic compression of the unburnt reactants. Reaction rates tend to increase with increasing reactant temperature. Similarly, combustion products are compressed isentropically with time, producing a temperature profile in the burnt products which is hottest at the center.

It is important to note that the reactants are compressed isentropically first and then irreversibly burned while the burnt products are irreversibly produced first and then isentropically compressed.

Figure 2: 20 liter dust sphere

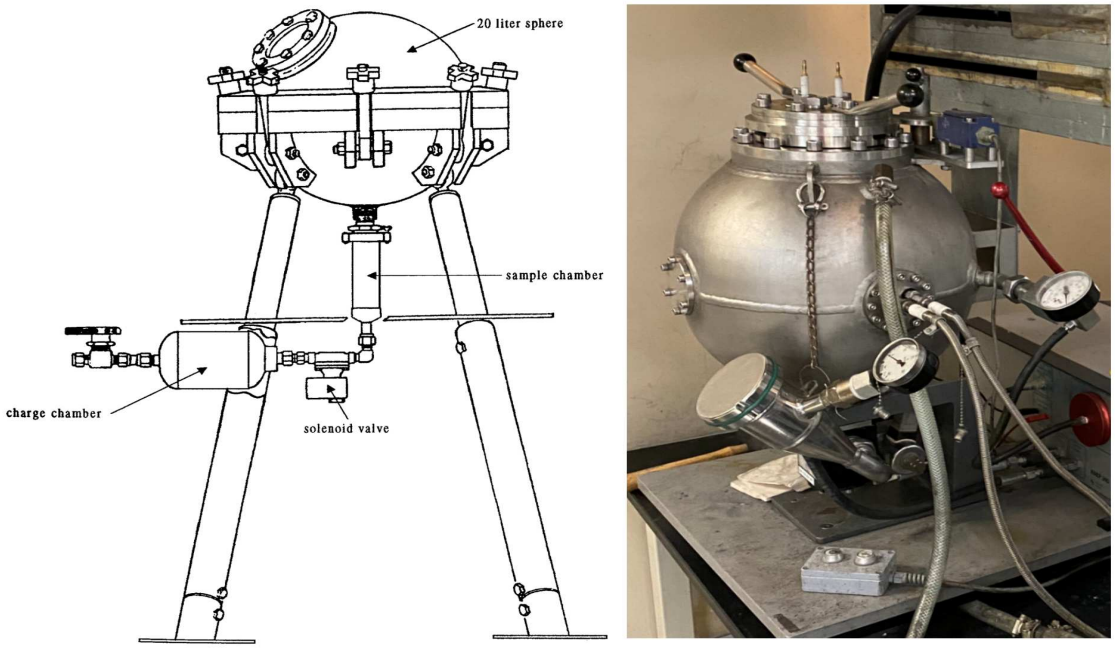

Courtesy of ioKinetic LLC.

This yields a higher level of specific entropy at the center than at the walls of the vessel. During combustion, pressure equalizes throughout the vessel at the speed of sound and flame propagation is similar to propagation in a constant pressure environment.

7 Detailed Modeling of Deflagration Venting Dynamics

We use a detailed one-dimensional model for the prediction of deflagration dynamics for mixtures of gases and dusts in cubic, rectangular, and spherical geometries. The non-ideal behavior of burnt and unburnt gaseous components is accounted for during combustion and venting. Detailed chemical equilibrium [2, 3, 4] calculations are used at every time step to represent the stoichiometry of the reactions as temperature and pressure change in the explosion volume. This model is implemented in SuperChems Expert™ (a component of Process Safety Office®). In the derivation and formulation of this model, the following assumptions are made:

- The gas and/or dust mixture is uniform in composition.
- The thickness of the flame in the reaction zone is negligible.
- The reaction products are calculated at every time step using direct minimization of the Gibbs free energy [2, 3, 4].
- The burning rate accelerates when the flame front becomes wrinkled at a critical expansion ratio corresponding to a critical Reynolds number.

Figure 3: Typical pressure history for strong flame-vent interaction

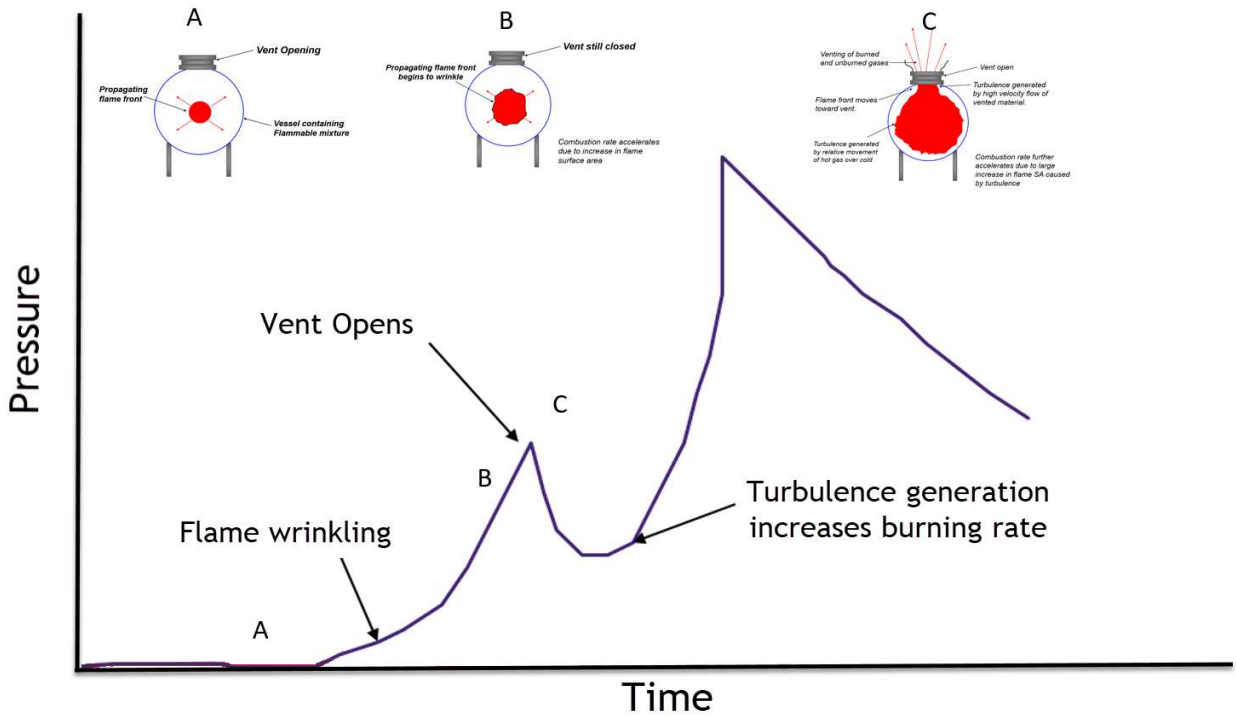

- Burnt and unburnt gases are treated assuming non-ideal gas behavior using a modified cubic equation of state [9].
- When venting occurs and depending on the location of the vent relative to the flame front, unburnt, burnt, or a mixture of burnt and unburnt materials is vented.
- The deflagration process is rapid, and therefore the only heat loss mechanism considered is radiation to the vessel walls from combustion products.
- The pressure is uniform in the vessel.
- The burnt and unburnt materials are compressed isentropically.

The rate of production of burnt material by the advancing flame front is calculated from:

$$\frac{dm_T}{dt} = A_f \rho_u s_f = A_f \rho_u s_u (\eta + \chi) \tag{12}$$

Where A_f is the flame surface area, s_f is the burning velocity, s_u is the laminar burning velocity, χ is a turbulence factor which accounts for vent opening dynamics, and η takes into account the increase in flame surface area due to cell formation. Correction for flame acceleration due to turbulence and instability effects is calculated by multiplying s_u by $(\eta + \chi)$.

Materials are incrementally reacted at the rate provided by Equation 12 using direct minimization of the Gibbs free energy. The final conditions are determined by solving for the pressure that satisfies the energy and mass balance constraints at constant volume. The constant volume constraint

is expressed as follows:

$$V_u\beta_u\frac{dT_u}{dt}+V_b\beta_b\frac{dT_b}{dt}-\left(V_u\kappa_u+V_b\kappa_b\right)\frac{dP}{dt}+\sum_i^r\overline{V}_{u_i}\frac{dN_i}{dt}+\sum_i^p\overline{V}_{b_i}\frac{dn_i}{dt} \;=\; 0 \tag{13}$$

where κ is the isothermal compressibility, β is the volume expansion coefficient, and $\overline{V}$ is the partial molar volume.

8 Burning Rate Model Development and Fitting

In general the laminar burning velocity can be represented using a power law function of pressure and temperature [10, 11]:

$$s_u \;=\; s_{u_o}\left[\frac{T}{T_o}\right]^{\alpha}\left[\frac{P}{P_o}\right]^{\beta}\left(1.0-2.1Y_{dil}\right) \;\text{ for }\; P\geq P_o \tag{14}$$

$$s_{u_o} \;=\; B_m+B_\phi\left(\phi-\phi_m\right)^2 \tag{15}$$

$$\alpha \;=\; 2.18-0.8\left(\phi-1\right) \tag{16}$$

$$\beta \;=\; -0.17+0.22\left(\phi-1\right) \tag{17}$$

$$\phi \;=\; \frac{\left[\frac{M_{fuel}}{M_{oxidizer}}\right]_{actual}}{\left[\frac{M_{fuel}}{M_{oxidizer}}\right]_{stoichiometric}}=\frac{\left[\frac{N_{fuel}}{N_{oxidizer}}\right]_{actual}}{\left[\frac{N_{fuel}}{N_{oxidizer}}\right]_{stoichiometric}} \tag{18}$$

where s_{u_o} is the reference laminar burning velocity, P_o and T_o are the reference temperature and pressure in absolute units, ϕ is the equivalence ratio, B_m is maximum flame speed attained at equivalence ratio ϕ_m, B_ϕ quantifies the dependence of flame speed on equivalence ratio, Y_{dil} is the mass fraction of diluent, α is the temperature exponent, and β is the pressure exponent. Typically, $\alpha=2.18$ and $\beta=-0.17$ are representative of most hydrocarbon fuels pressure and temperature dependency. Data for laminar burning velocity for a wide variety of fuels is provided in Tables 3 and Tables 6 to 10.

The flame burning velocity form used in our model is the one reported by Chippett [12]:

$$s_f \;=\; \left(\chi+\eta\right)s_u=\left(\chi+\eta\right)s_{u_o}\left[\frac{T_u}{T_o}\right]^{\alpha}\left[\frac{P}{P_o}\right]^{\beta} \tag{19}$$

The factor χ is a turbulence factor which accounts for vent opening dynamics. Its value changes with time [13, 14] and typically ranges from 1.5 to 10:

Turbulence is not present prior to ignition: For large enclosures (room or laboratory size) where turbulence is generated by furniture and obstacles present on one level a value of χ of 1.5 is recommended. For explosions propagating through large openings into other sections of an enclosure or where obstacles are distributed throughout the entire volume use a χ value of 5.

Turbulence is present prior to ignition: Use a value χ ranging from 8 to 10.

The sudden opening of a vent (rupture disk, for example) can produce an acoustic wave (pressure) which initiates a hydrodynamic instability within the flame front. Suggested χ values (based on experimental data) for use with the above equation are:

Initially open vent χ ranges from 1 to 2

Initially closed vent χ ranges from 3 to 5

The lower value of χ is recommended if the value of s_{u_o} is less than 0.5 m/s, otherwise the higher χ value should be used.

The factor η takes into account the increase in flame surface area due to cell formation and is estimated by:

$$\eta = \left(\frac{N_{Pr} N_{Re}}{N_{Pr_c} N_{Re_c}} \right)^{\theta} \tag{20}$$

where, N_{Re} is the flame Reynolds number and is given by:

$$N_{Re} = \frac{\rho_u r_b s_{u_o}}{\mu_u} \tag{21}$$

where N_{Re} is the Reynolds number, N_{Pr} is the Prandtl number, r_b is the flame radius, and μ is the viscosity. The value of η is greater than or equal to unity. The product $N_{Pr_c} N_{Re_c}$ is the flame stability parameter used by Istratov and Librovich [15]. Typical combustion conditions indicate that values of N_{Pr_c} are close to one. In this case, the onset of cell formation may be predicted by using the data of Groff [16]:

$$N_{Re_c} = 155555 \frac{\rho_b}{\rho_u} - 16667 \tag{22}$$

The exponent, θ was experimentally determined by Chippett [12] from comparisons of closed vessel time-pressure curves for propane and methane in spherical vessels ranging in size from 0.005 to 3.8 m^3. He reported a value of 0.4 for methane and 0.25 for propane (see Table 3).

Table 3: Burning velocity model parameters for different fuels

Chemical	s_{u_o}, $\mathrm{m/s}$	α	β	θ	Reference
Methane	0.33	2.00	-0.25	0.40	[12]
Propane	0.32	2.13	-0.17	0.25	[12]
Pentane	0.50	1.60	-0.25	0.39	[10], [11], [17]
Acetylene	1.58	2.00	-0.06	0.39	[10], [11], [17]
Hydrogen	3.50	1.26	0.26	0.39	[10], [11], [17]
Methanol	0.37	2.18	-0.16	0.39	[10], [11], [17]
isoOctane	0.26	2.18	-0.16	0.39	[10], [11], [17]

Equation 19 is valid at low length to diameter ratios ($L/D \simeq 1$). For elongated geometries, flame acceleration due to flow turbulence and the presence of obstructions can lead to much higher burning velocities ([18, 19, 20]). For large L/D ratios, a deflagration to detonation transition (DDT) can occur. Numerous empirical and semi-empirical correlations for flame acceleration in pipes have appeared in the literature. Many of these correlations relate flame acceleration to L/D ratio. A

simple correlation for ducts or pipes without obstructions (smooth pipe) that is based on measured flame acceleration data for hydrogen, methane, propane, and ethylene was proposed by [18]:

$$\frac{s_f(x)}{s_u} = 6.5\sigma \exp\left[0.0061\left(\sigma-1\right)\left(\frac{x}{D}\right)\left(\frac{D}{0.15}\right)^{0.4}\right] \tag{23}$$

$$\sigma = \frac{\rho_u}{\rho_b} \tag{24}$$

where s_u is the laminar burning velocity, 0.15 is the reference diameter in meters, σ is the expansion ratio of the combustion products, x is the position of the flame, D is the diameter of the duct or pipe, and $s_f(x)$ is the flame speed at location x.

If we assume that a deflagration to detonation transition occurs when the flame speed $s_f(x)$ reaches 1/2 of the Chapman-Jouguet detonation velocity u_{CJ}, we can solve the above equation for the x/D ratio at which DDT occurs [18]:

$$\frac{1}{2}u_{CJ} = s_f(x) \quad \text{or} \tag{25}$$

$$\left[\frac{x}{D}\right]_{\text{DDT,smooth}} = \frac{1}{0.0061\left(\sigma-1\right)}\left(\frac{0.15}{D}\right)^{0.4}\ln\left(0.077\frac{u_{CJ}}{\sigma s_u}\right) \tag{26}$$

Using a laminar burning velocity value of 2.3 m/s, an expansion ratio of 7, a pipe diameter of 0.15 m, and a detonation velocity of 1263 m/s for a mixture of 10 % mole fraction hydrogen in air, the above equation yields an x/D for DDT transition of:

$$\left[\frac{x}{D}\right]_{\text{DDT,smooth}} = \frac{1}{0.0061\left(7-1\right)}\left(\frac{0.15}{0.15}\right)^{0.4}\ln\left(0.077\frac{1263}{7\times 2.3}\right) = 49.13 \tag{27}$$

or 7.37 meters. For obstructed ducts, reference [18] recommends the following expression for x/D as a function of blockage ratio (BR) which is a representation of how much of the flow area is blocked:

$$\left[\frac{x}{D}\right]_{\text{DDT}} = \frac{1}{1+15BR}\left[\frac{x}{D}\right]_{\text{DDT,smooth}} \tag{28}$$

where the maximum BR value to be used is 0.6 approximately. At a blockage ratio of 0.5, the above equation yields an x/D of 5.78 or an actual length of 0.86 meters. Equation 23 can then be adjusted to reflect the influence of blockage on flame acceleration:

$$\frac{s_f(x)}{s_u} = 6.5\sigma \exp\left[0.0061\left(\sigma-1\right)\left(1+15BR\right)\left(\frac{x}{D}\right)\left(\frac{D}{0.15}\right)^{0.4}\right] \tag{29}$$

Excellent agreement for flame acceleration is reported for Equation 23 by Silvestrini et al. [18] for hydrogen, methane, ethylene, and propane in tubes ranging from 0.15 to 1.4 meters in diameter as shown in Figures 4 and 5.

Figure 4: Flame speed of flammable materials in a 0.15 m diameter tube [18]

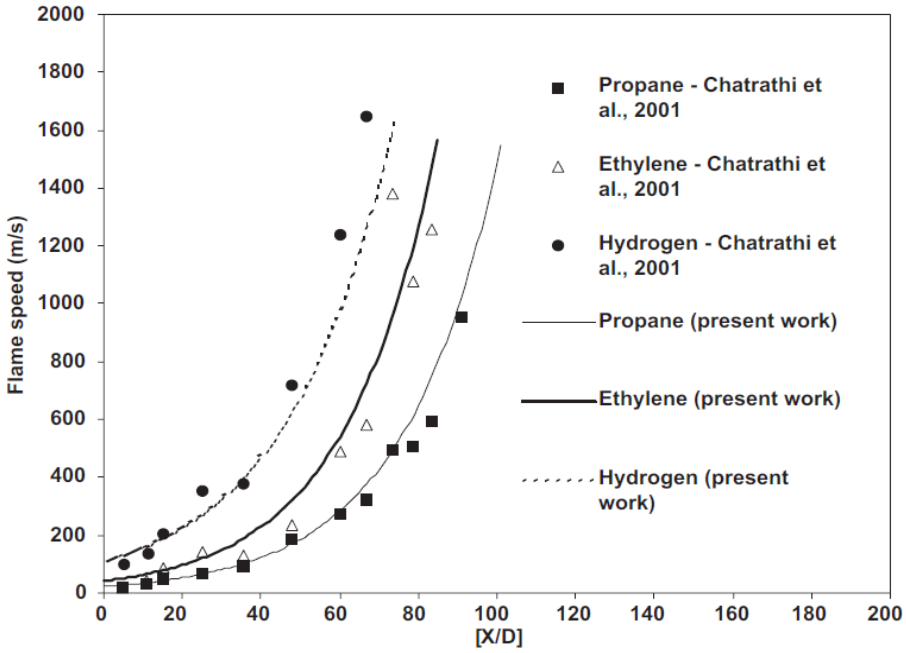

9 Estimation of Energy Loss to Vessel Walls

The total energy loss from the combustion reaction includes heat radiated from the hot products to the vessel walls as well as heat lost by convection and conduction from products and reactants.

The radiant heat loss rate to the vessel walls is calculated from [21]:

$$\frac{dQ_r}{dt} = -\frac{\sigma A_f \left[T_b^4 - T_w^4\right]}{\frac{1}{\epsilon_b} + \left(\frac{A_f}{A_w}\right)\left(\frac{1}{\alpha_w} - 1\right)} \tag{30}$$

where, A_w is the internal vessel wall surface area, T_w is the average vessel walls temperature, σ is Boltzman's constant which is equal to 5.67×10^{-8}, $\mathrm{W/m^2/K^4}$, α_w is the absorptivity at the wall, and ϵ_b is the emissivity of combustion products.

The emissivity of combustion products may be estimated using Schack's equation [22]:

$$\epsilon_b = 0.7\sqrt{\frac{100 p_{CO_2} L}{T_b}} + \frac{700\left(p_{H_2O} L\right)^{0.8}}{T_b} \tag{31}$$

$$L = \frac{4V_b}{A_w} \tag{32}$$

where, p_{CO_2} is the partial pressure of carbon dioxide in combustion products in atm, p_{H_2O} is the partial pressure of water vapor in combustion products in atm, and L is the effective depth of the radiative gas layer in m.

The convective contribution to the total combustion heat losses may be neglected because of the short duration of the explosion process [23]. The conductive heat losses may be neglected since the flame touches the wall in the latter part of the combustion reaction.

Figure 5: Comparison between measured and calculated flame speeds [18] using Equation 23

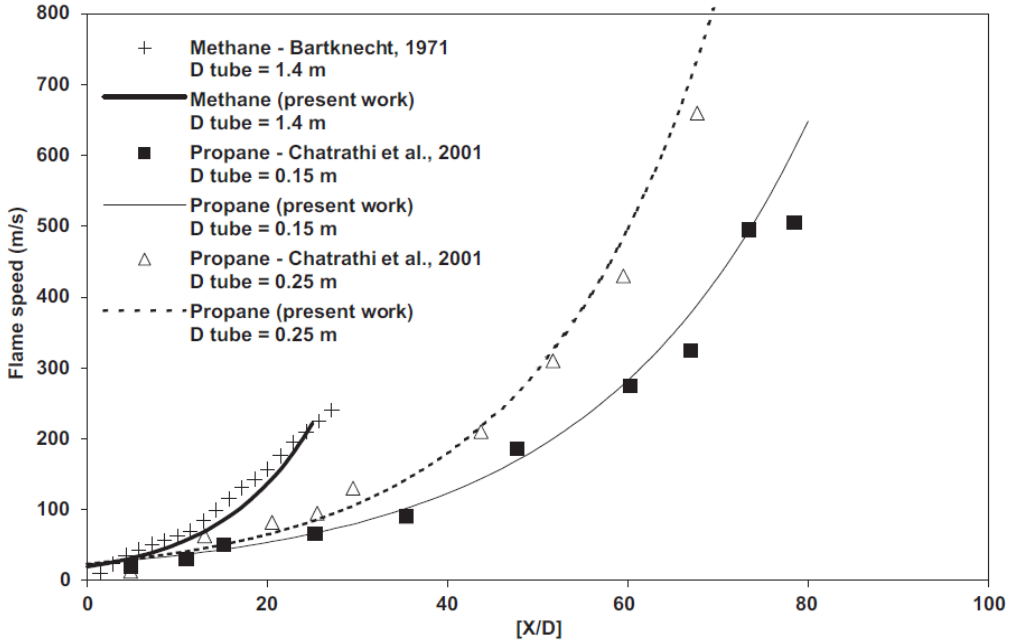

10 Case Study - Energetic Dust Burning Rate Model Development

The deflagration dynamics model described earlier can be used to fit the parameters of a general burning rate model from measured 20 liter test data. Once the burning rate model parameters are established, they can be used to develop relief requirements for elevated initial pressures and/or temperatures. This is only possible because of the detailed chemical equilibrium estimates for reaction stoichiometry and energetics conducted at every time step during the transient simulation. This process is similar in concept to the development of global kinetic models for condensed phase runaway reactions from calorimetry data.

Dust test data was obtained in a 20 liter sphere of an energetic dust material mixed with other inert materials. The data reported included K_{st}, P_{max}, and dP/dt as a function of time. Multiple data sets were obtained at 500, 750, and 1000 $\mathrm{g/m^3}$ dust concentrations. The test data was obtained using starting conditions of 25 C and 1 bara. The test data was then simulated with SuperChems Expert to develop a burning rate model that can be used to extrapolate the measured data to elevated initial temperatures and/or pressures as well as other concentration ranges. A comparison between measured and simulated data is provided in Table 4.

Excellent agreement is observed between measurements and burning rate model predictions. The measured data contains several fuel rich concentrations of dust (see Figures 6 and 7). The model best fit for burning velocity is therefore developed as a function of equivalence ratio:

$$s_{u_o} = 0.8 + 0.67\phi \tag{33}$$

A burning rate model, when coupled with detailed chemical equilibrium calculations, can extend the applicability and usability of the test data. In this case study, an initial process temperature

Table 4: Summary of measured vs. SuperChems Expert predicted data

	Material A Concentation (g/m3)	Material B Concentration (g/m3)	Material B Mass (g)	Pmax (bar)	dP/dt (bar/s)	Kst (bar.m/s)	Equivalence Ratio	Sfo	Flame Temperature (C)
Measured	500	200	3.937	6.88	2274	617			
Predicted				7.73	2325	627	1.966	2.10	1383
Measured	750	300	5.905	7.04	2628	713			
Predicted				6.95	2623	709	2.946	2.75	1234
Mesured	1000	400	7.874	6.93	2995	813			
Predicted				6.92	3041	821	3.704	3.25	1158

of 300 C is used to develop the explosion relief requirements as shown in Figure 8. The venting requirements considered two 10 cm OD open pipes and a dust concentration of 100 $\mathrm{g/m^3}$.

11 Case Study - Deflagration Venting for Large-Scale Battery Energy Storage Systems

Lithium ion batteries represent a large market share of the overall electrochemical energy storage capacity in the USA. It is estimated at approximately 80 % of 1.2 GW [2]. Other large energy storage systems (ESS) technologies are also gaining popularity such as flow batteries.

Whenever we have a system that has a large energy density storage, runaway reactions become a concern. Runaway reactions can produce excessive amounts of heating, pressure, and can also create toxicity exposure due to the nature of the battery materials decomposition and combustion products. Some of the battery material decomposition products may include toxic chemicals such as hydrogen fluoride.

A variety of tests are used to induce battery failures and to measure their heat and pressure release rates. Recent test data by UL laboratories [24] shows that production of flammable gases occurs during a thermal runaway including CO, $\mathrm{CO_2}$, $\mathrm{O_2}$, $\mathrm{H_2}$, and $\mathrm{CH_4}$ (see Figure 9). The decomposition products represent a deflagration potential. Depending on the composition of hydrogen, a deflagration to detonation transition or a prompt detonation may also be possible.

The data provided by UL in Figure 9 can be used to design adequate deflagration venting using SuperChems Expert . This is possible because of how SuperChems Expert automatically calculates the combustion stoichiometry and equilibrium products and energetics at every time step as shown to the right.

```
+0.857 CO2 +0.143 CH4 +0.286 N2 <---> + C +0.571 HNO3
+0.929 CO2 +0.0714 CH4 +0.143 N2 <---> + CO +0.286 HNO3
+0.143 CO2 +0.571 HNO3 <---> +0.143 CH4 +0.286 N2 + O2
+0.357 CH4 +0.571 HNO3 <---> +0.357 CO2 +0.286 N2 + H2O
+0.643 CH4 +0.286 N2 +0.429 HNO3 <---> +0.643 CO2 + H3N
+0.0714 CO2 +0.357 N2 +0.286 HNO3 <---> +0.0714 CH4 + NO
+0.143 CO2 +0.214 N2 +0.571 HNO3 <---> +0.143 CH4 + NO2
+0.143 CH4 +0.429 HNO3 <---> +0.143 CO2 +0.214 N2 + OH
+0.214 CH4 +0.143 HNO3 <---> +0.214 CO2 +0.0714 N2 + H
+0.0714 CO2 +0.286 HNO3 <---> +0.0714 CH4 +0.143 N2 + O
+0.5 N2 <---> + N
+0.429 CH4 +0.286 HNO3 <---> + H2 +0.429 CO2 +0.143 N2
```

[2] U.S. Energy Information Administration. U.S. Battery Market Storage Trends. May 2018

Figure 6: Measured vs. predicted P_{max} values using SuperChems Expert

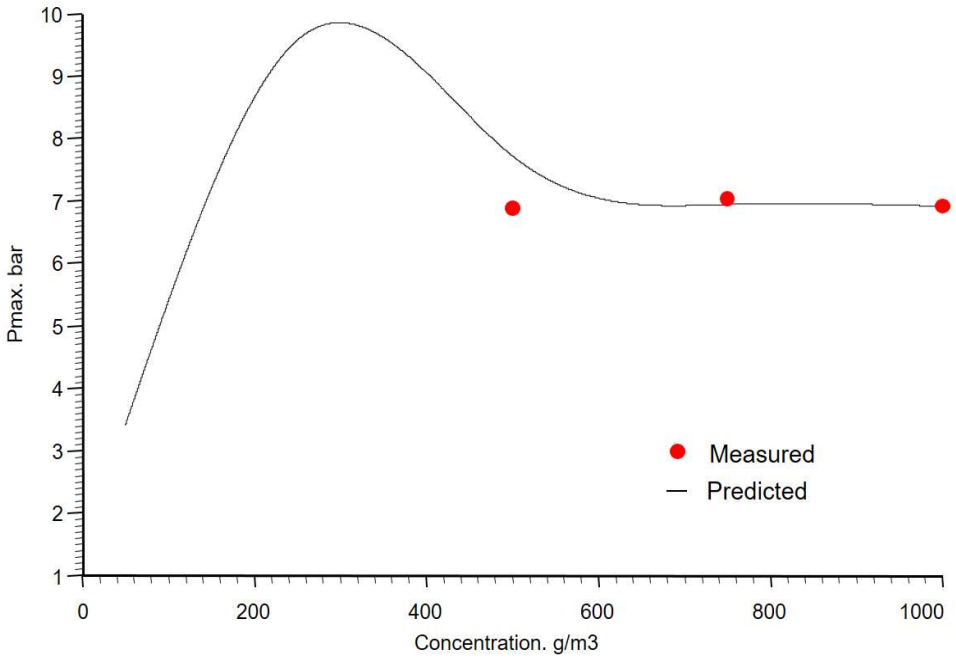

The data measured by UL provides the relative composition of the thermal runaway products. These products include 22.1 % of carbon dioxide which acts as a diluent. In addition UL reports the burning velocity at 0.35 m/s for the mixture and a maximum pressure of 91 psig without venting. They also report a lower flammable limit of 8.5 %. If we ignore flame acceleration we can use their measurements to create a burning rate model for the mixture:

$$s_{u_o} = 0.35 \tag{34}$$

$$s_f = (\chi + \eta)\, s_{u_o} \left[\frac{T_u}{T_o}\right]^{2.18} \left[\frac{P}{P_o}\right]^{-0.17} \tag{35}$$

First, chemical equilibrium Rankine-Hugoniot estimates are performed to find the Chapman-Jouguet (CJ) conditions for a strong detonation (upper) and a strong deflagration (lower) and to determine the constant volume pressure and temperature conditions as well as the constant pressure theoretical flame temperature. This is shown in Figure 10 for the UL measured composition at near stoichiometric conditions with air. The maximum pressure at constant volume is consistent with the measured pressure by UL, 99 psig vs. 91 psig.

To illustrate the use of the above burning rate model and the detailed chemical equilibrium transient estimates, we consider a 33 m^3 ESS enclosure that is full of a stoichiometric mixture of the UL measured decomposition products and air. We also consider that a deflagration occurs at a starting temperature of 100 C and 0 psig and that the ESS is outfitted with two fast acting rupture disks set at 1.5 psig with a total flow area of 22.5 ft^2. Figure 11 confirms that 22.5 ft^2 of deflagration venting will keep the ESS overpressure to 1.5 psig or less. During the deflagration a mixture of both unburnt reactants and combustion products is vented. A discharge coefficient of 0.6 is used for the rupture disks and no flame acceleration due the opening of the rupture disks is used.

SuperChems Expert also includes one dimensional (1D) explosion gas dynamics models for piping

Figure 7: Measured vs. predicted dP/dt values using SuperChems Expert

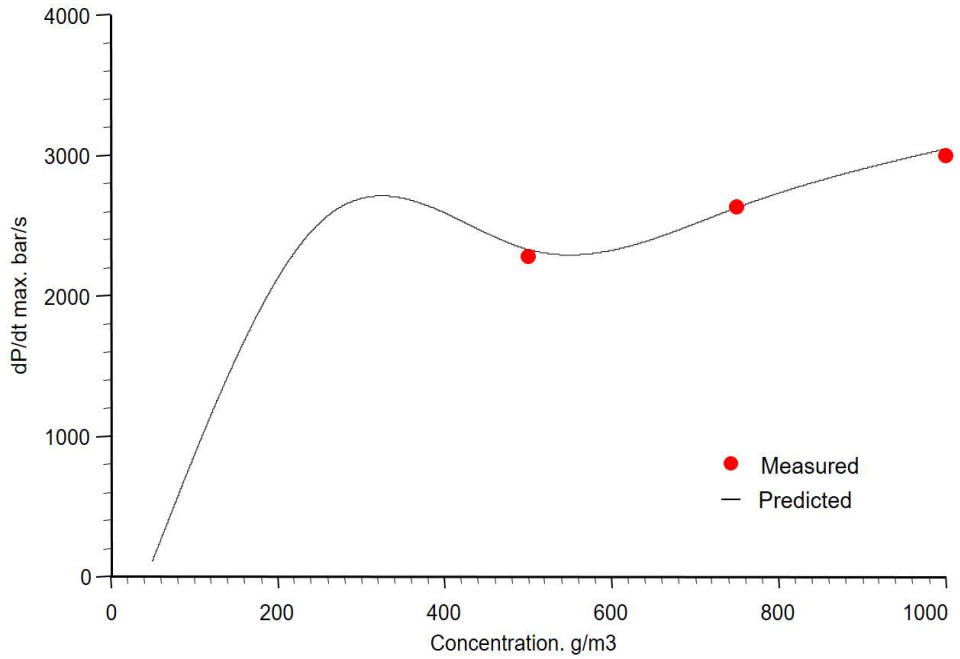

and elongated enclosures. These models use a solid flame model coupled with the Eulerian gas dynamics to determine the time history of pressure, temperature, and venting rate.

12 Pressure Pileup Considerations

Pressure pileup can occur when deflagrations occur in interconnected vessels and enclosures. As the flames burn in one vessel or enclosure, the materials in connected vessels get compressed. This compression leads to higher initial pressures and temperatures in the connected vessels or enclosures leading to faster combustion and higher pressures and pressure rates in those vessels.

Figure 12 illustrates a deflagration on compartment A that is venting into compartment B. This venting arrangement is sometimes encountered in facilities and can be very hazardous, especially if compartment B contains a flammable mixture. During a deflagration in compartment A, the pressure in compartment B is increased by the expanding combustion products in compartment A. Figure 13 shows a typical pressure pileup condition where pressure in the secondary chamber (red) raises steadily until the flame arrives and a very fast combustion occurs [25].

The mixture in compartment B is compressed as a result. If ignited by the flame front from compartment A or due to autoignition, the pressures in compartment B can be substantial. The final pressure depends on the relative size of the compartments and the joining pipe diameter. In some cases, a deflagration to detonation transition (DDT) can occur.

Figure 8: Calculated equipment pressure profile during a dust explosion using SuperChems Expert

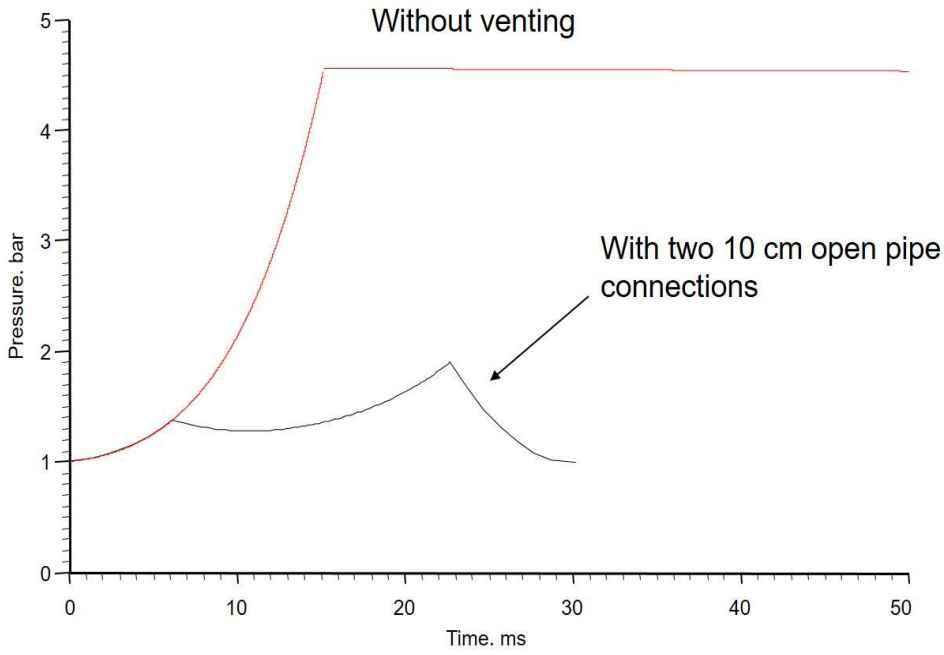

13 Understanding Dust Explosions and Hazards

Dust explosions occur when small particles of solid materials ($\leq$ 500 μm) [3] are dispersed in air and then ignited. Initial dust explosions are sometimes followed by secondary explosions which can be more damaging. The blast wave generated by the initial explosion disturbs and stirs additional dust which then result in secondary explosions if ignited. Ignition and flame propagation in dusts are a function of particle size, particle loading, and mixing conditions.

Even thin layers of dust can cause significant explosion hazards. A 1 mm dust layer with a bulk density of 500 $\mathrm{kg/m^3}$ can generate a dust cloud that is 5 meters high at a dust concentration of 100 $\mathrm{g/m^3}$ or 1 meter cloud at 500 $\mathrm{g/m^3}$:

$$C = 1000\rho_{bulk}\frac{h}{H} \tag{36}$$

where C is the dust concentration in $\mathrm{g/m^3}$, h is the dust layer thickness in meters, and H is the dust cloud height in meters.

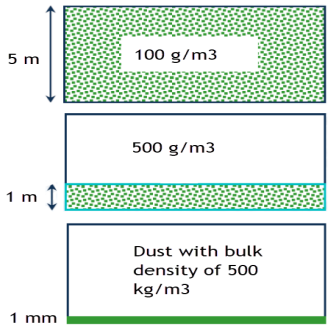

Figure 14 illustrates a typical range of dust concentrations in air at ambient temperature and pressure. Limits associated with permissible dust exposure from an industrial hygiene perspective are much smaller than what is required for an explosive dust concentration or dust layer deposit.

Dusts are classified as St-0 (no Explosion), St-1 (weak explosion), St-2 (strong explosion), or St-3 (very strong explosion) dusts based on the value of their deflagration index. For St-1 dusts $1 \leq K_{st} < 201$, for St-2 dusts $201 \leq K_{st} < 300$ and for St-3 dusts $K_{st} \geq 300$.

[3] A human hair ranges in size from 50 to 200 μm

Figure 9: Lithium ion battery thermal runaway decomposition products [24]

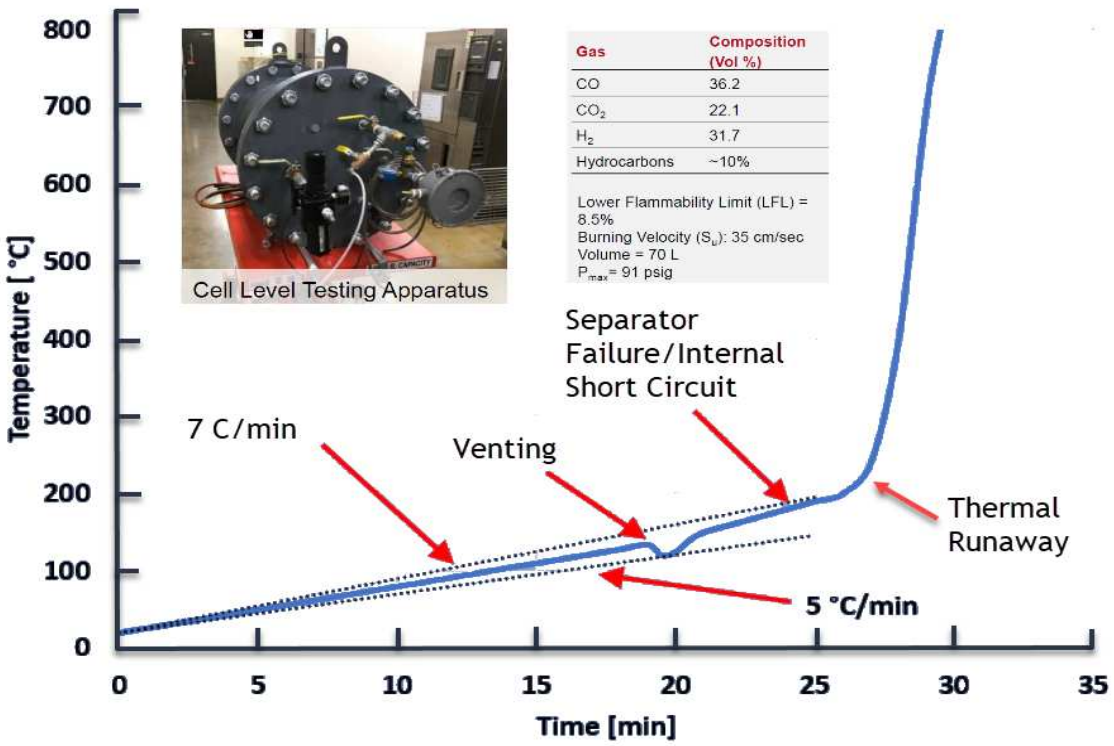

Characterization of dust hazards typically involves measurement of one or more of the properties shown in Table 5. For proper evaluation of dust hazards, properties a-g must be determined as a minimum. For dusts with an MIE of 10 mJ or less, property h should also be obtained, as inerting may be necessary. For systems that supply or generate heat (e.g., driers, mills, and self heating products), properties i-k must also be obtained.

More confidence in managing dust hazards can be achieved when measurements are provided for actual dust samples. The properties shown in Table 5 can help to answer questions about the likelihood of ignition, what happens if the dust ignites, and the requirements for venting and avoidance of flammable atmospheres. Guidance for managing dusts potential hazards [27] is provided in Figure 15 as a function of dust sensitivity and ignition source intensity.

14 Conclusions

We have demonstrated how detailed modeling of deflagration and venting dynamics integrates direct Gibbs free energy minimization (thermodynamics) with burning rate models (kinetics) based on either measured or published explosion severity data. This method was implemented in SuperChems Expert in the early 1990s and has proven to be more versatile, useful, and reliable than simplified methods.

The SuperChems Expert implementation overcomes simplified methods shortcomings including but not limited to systems with elevated initial temperatures or pressures, hybrid systems containing flammable gases and dusts, systems with diluents and/or chemical oxidizers, systems with

Figure 10: Chapman-Jouguet (CJ) conditions for battery thermal decomposition products

Hugoniot

Summary | Profiles

	A	B	C	D	E	F	G
1	**HUGONIOT / TEST BATTERY MIXTURE FLAMMABILITY COPY						
2							
3		INITIAL CONDITIONS	CONSTANT PRESSURE	CONSTANT VOLUME	UPPER CJ	LOWER CJ	MW
4	HYDROGEN. kmol	0.3170	0.0071	0.0113	0.0150	0.0039	2.0159
5	CARBON DIOXIDE. kmol	0.2210	0.6368	0.6001	0.5694	0.6604	44.0098
6	CARBON MONOXIDE. kmol	0.3620	0.0462	0.0829	0.1136	0.0226	28.0104
7	METHANE. kmol	0.1000	0.0000	0.0000	0.0000	0.0000	16.0428
8	NITROGEN. kmol	2.0303	2.0269	2.0223	2.0183	2.0288	28.0135
9	OXYGEN. kmol	0.5397	0.0211	0.0343	0.0449	0.0110	31.9988
10	WATER. kmol		0.5051	0.4959	0.4874	0.5111	18.0153
11	AMMONIA. kmol		0.0000	0.0000	0.0000	0.0000	17.0306
12	NITRIC OXIDE. kmol		0.0068	0.0160	0.0240	0.0030	30.0061
13	NITROGEN DIOXIDE. kmol		0.0000	0.0000	0.0000	0.0000	46.0055
14	HYDROXYL. kmol		0.0086	0.0178	0.0262	0.0038	17.0073
15	MONOATOMIC HYDROGEN. kmol		0.0009	0.0019	0.0031	0.0003	1.0079
16	MONOATOMIC OXYGEN. kmol		0.0007	0.0020	0.0036	0.0002	15.9994
17	NITROGEN RADICAL. kmol		0.0000	0.0000	0.0000	0.0000	14.0067
18	NITRIC ACID. kmol		0.0000	0.0000	0.0000	0.0000	63.0129
19							
20	CARBON-REF. kmol		0.0000	0.0000	0.0000	0.0000	12.0110
21							
22	Temperature. C	25.0000	1925.3414	2244.1801	2414.5903	1730.0701	
23	Pressure. psig			99.4600	206.9148	-8.1877	
24							
25	T/To		7.3738	8.4432	9.0147	6.7188	
26	P/Po		1.0000	7.7679	15.0797	0.4429	
27							
28	Total mass. kg	96.2548	96.2548	96.2548	96.2548	96.2548	
29	Total volume. m3	87.3400	588.1558	87.3401	48.3431	1204.4537	
30	Total enthalpy. J	-134464856.4640	-134452140.8512	-74552747.5697	-37681828.6597	-170923883.2997	
31	Total entropy. J/C	24933.7997	224694.1104	192086.4604	186362.3566	230999.1436	
32							
33	Speed of sound in gas. m/s	357.2074	874.4519	938.6960	973.3065	833.2987	
34	Particle velocity. m/s				942.4615	872.7113	
35	Shock velocity. m/s				1702.7162	63.2840	
36							
37	Last Executed: 01:57:35 PM, Fri Feb 14 2020						
38							

reduced venting set pressures, geometries with long L/D ratios or geometries with long vent piping where flame acceleration becomes significant.

By using direct Gibbs free energy minimization, SuperChems Expert provides complete and detailed Rankine-Hugoniot combustion curves that yield upper and lower CJ conditions (see 10) and working fluid heat addition models. These combustion models are used to model the one-dimensional (1D) explosion dynamics in complex piping and elongated enclosures. SuperChems Expert uses a solid flame model coupled with 1D Eulerian gas dynamics to determine the time history of pressure, temperature, and venting rate in complex piping geometries and elongated enclosures.

Figure 11: Deflagration venting dynamics for 33 m^3 ESS

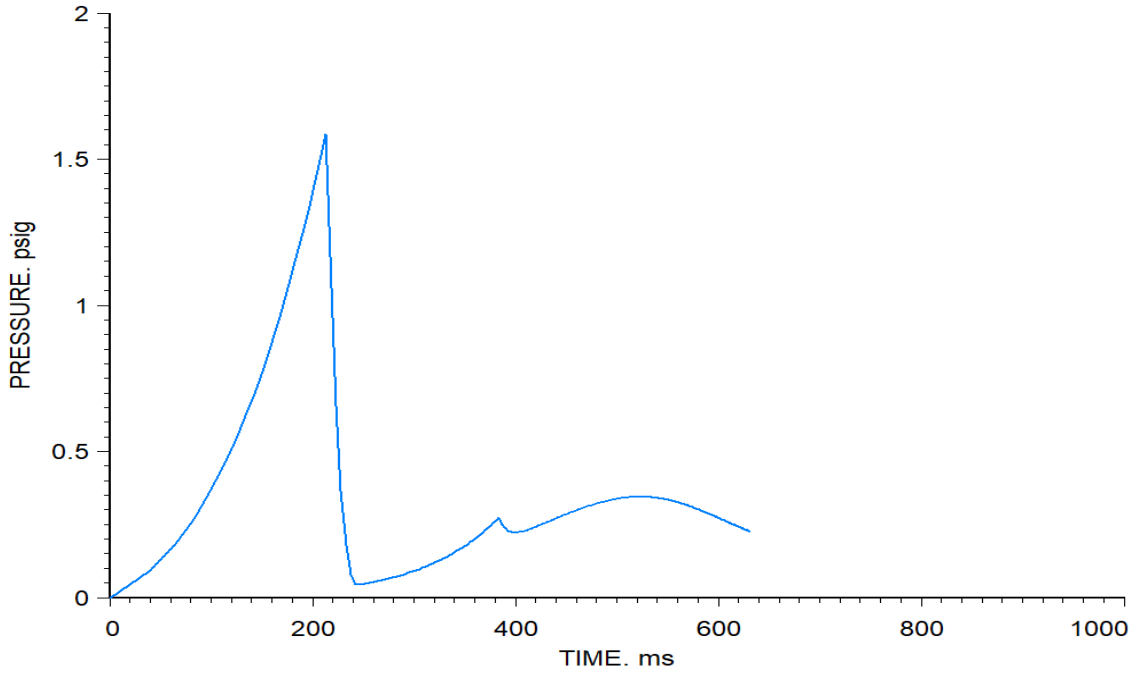

Figure 12: Pressure pileup during a deflagration

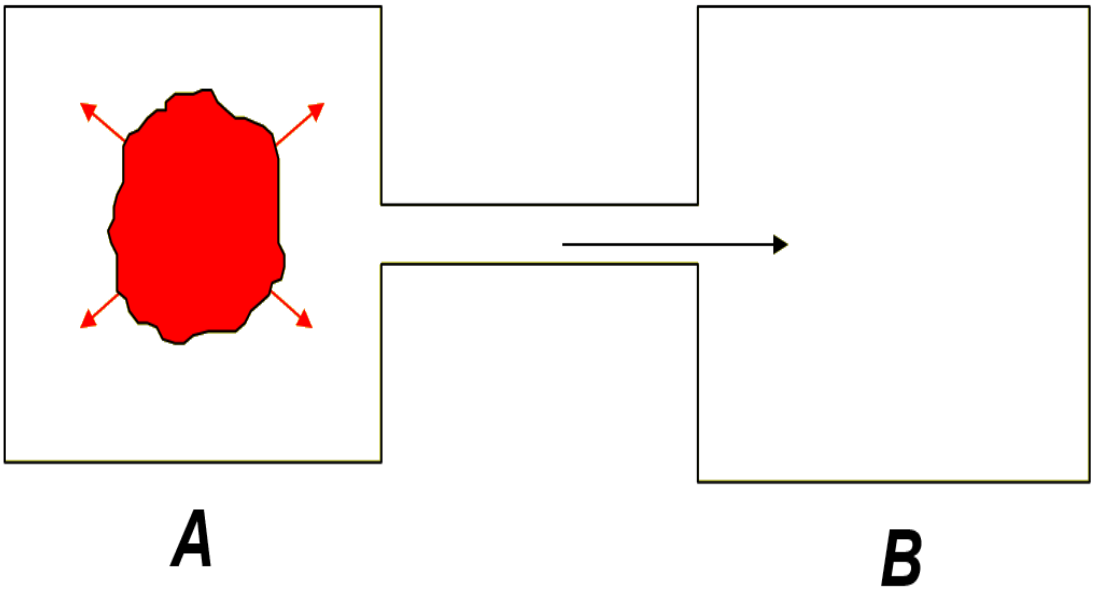

Figure 13: Measured pressure pileup history during a deflagration [25]

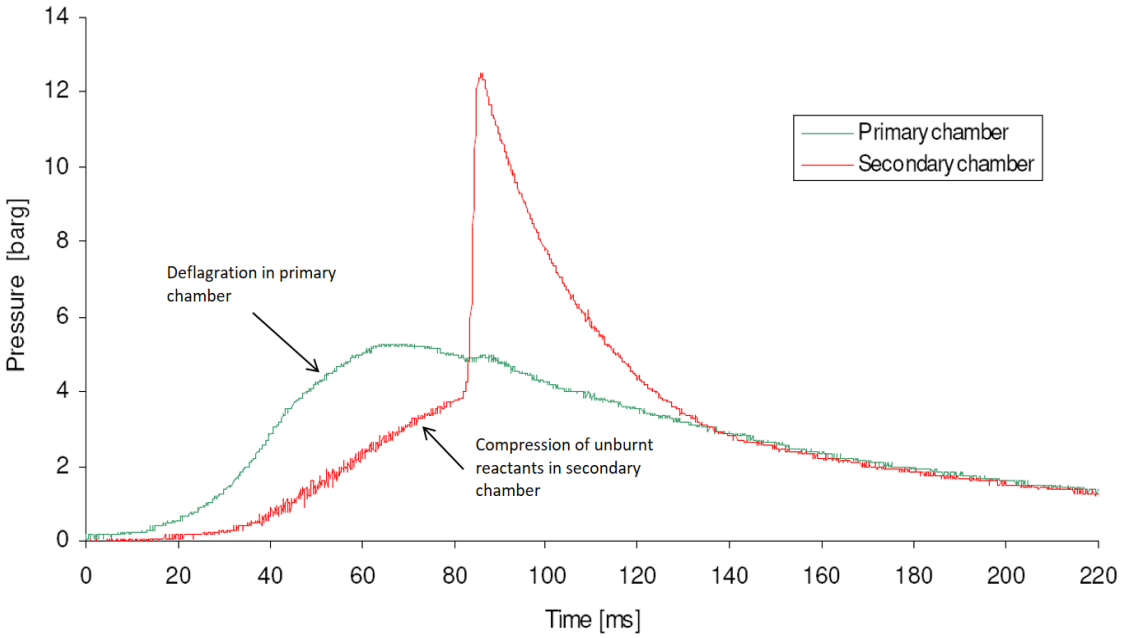

Figure 14: Typical range of explosive dust concentrations for maize starch [26]

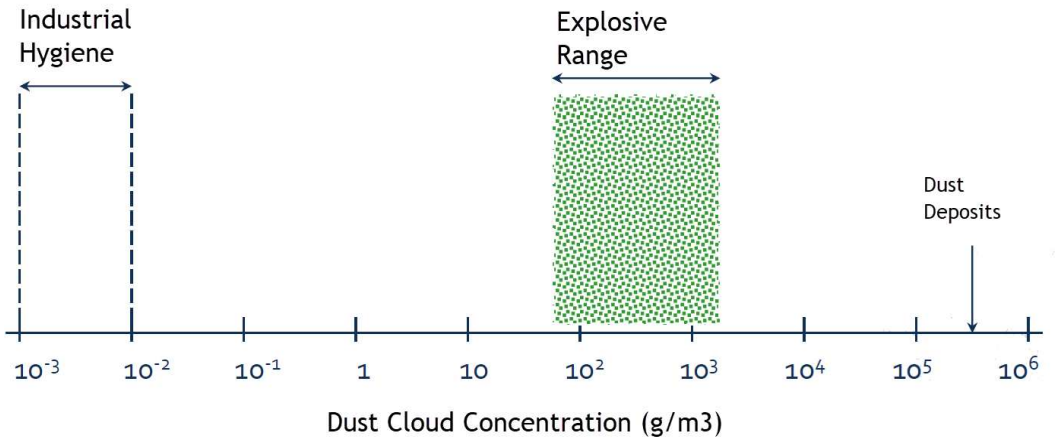

Table 5: Dust data requirements for proper hazard evaluation

#	**Property**	**Unit**	**Standards**
a	Particle size and particle size distribution, d	μm	
b	Water content of the powder, WC	% (w/w)	
c	Lower explosion limit, LEL or Minimum Explosive Concentration, MEC	g/m^3 or % (v/v)	ASTM E1515, EN 14034-2/ISO-6184
d	Maximum explosion pressure, P_{max}	barg	
e	Explosion severity index, K_{st}	bar.m/s	ASTM E1226-12a, EN 14034-2/ISO-6184, EN 2011.
f	Minimum ignition energy, MIE	mJ	ASTM E2019, EN 13821
g	Minimum ignition temperature of dust cloud, MIT or MAIT	°C	ASTM E1491, IEC 61241-2-1
h	Limiting oxygen concentration, LOC	% (v/v)	ASTM E2931, EN 14034-2
i	Minimum ignition temperature of a dust layer or smoldering temperature, LIT or ST	°C	ASTM E2021, IEC 61241
j	Autoignition temperature of a dust deposit, AIT	°C	
k	Burning behavior of a dust layer, BG		
l	Volume resistivity, capacity to store an electrostatic charge	Ωm	ASTM 61241-2-2, IEC 61241-2-2
m	Charge relaxation time taken to reach 37 % and 10 % of initial value	s	ASTM D257

Figure 15: Guidance for managing dusts potential hazards [27]

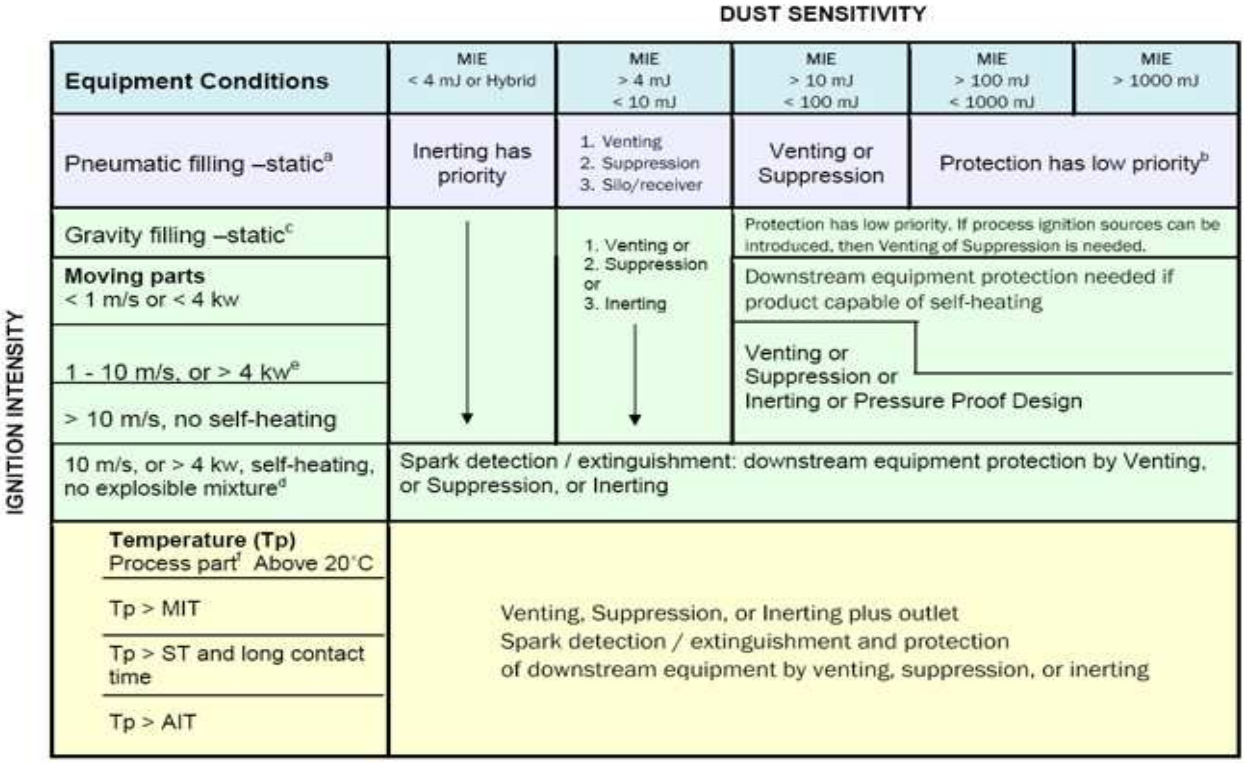

a Assumes all process components (silos, filters, cyclones, blenders, etc.) are made of metal and grounded and bonded. Flexible joints and filter bags are made of antistatic or conductive materials.

b The choice will depend on the explosion effects. If the effect is unacceptable, then the component should be protected.

c Filling the vessel from a rotary valve, fall pipe, transport conveyor, container, bag or large bag. All components except bags, are made of metal or antistatic or conductive materials and are adequately grounded and bonded.

d In some equipment (e.g., redlers and blenders with slowly moving parts) hardly any dust/air mixtures are produced. In other cases, explosive dust air mixtures should be expected unless proven otherwise.

e Only friction between CS and SS components considered. In case other materials are involved, the hazard should be evaluated further. Particular attention should be given to combinations of light metals with corroded steel, since the frictional sparks produced are intense ignition sources.

f The process could be a vessel wall, hot gases, hot product material (exothermic reactions) and hot probes, such as an oxygen analyzer. Direct fired product driers are not addressed here.

Table 6: Burning velocities of saturated hydrocarbons at 25 C air-fuel temperature and 1 atm (0.31 mole % H_2O in air) [28]

	Equivalence Ratio ϕ								S_u in cm/s		T and P Exponents	
Chemical	0.7	0.8	0.9	1.0	1.1	1.2	1.3	1.4	S_{max}	ϕ at S_{max}	α	β
Ethane	30.60	36.00	40.60	44.50	47.30	47.30	44.40	37.40	47.60	1.14	2.07	-0.14
	22.00	29.00	36.50	42.50	43.00	42.50	40.00	27.50				
Propane			42.30	45.60	46.20	42.40	34.30		46.40	1.06	2.13	-0.16
	24.00	32.00	39.50	44.00	45.00	43.50	37.00	28.00				
	23.00	30.00	37.00	39.00	41.00	40.50	33.50	25.00				
n-Butane		38.00	42.60	44.80	44.20	41.20	34.40	25.00	44.90	1.03	2.16	-0.16
Methane		30.00	38.30	43.40	44.70	39.80	31.20		44.80	1.08	2.12	-0.15
	20.50	28.00	36.00	40.50	42.00	37.00	27.00	17.50				
	17.00	25.00	33.00	38.00	38.50	34.00	24.00	13.50				
n-Pentane		35.00	40.50	42.70	42.70	39.30	33.90		43.00	1.05	2.14	-0.16
n-Heptane		37.00	39.80	42.20	42.00	35.50	29.40		42.80	1.05	2.14	-0.16
2,2,4-Trimethylpentane		37.50	40.20	41.00	37.20	31.00	23.50		41.00	0.98	2.20	-0.17
2,2,3-Trimethylpentane		37.80	39.50	40.10	39.50	36.20			40.10	1.00	2.18	-0.17
2,2-Dimethylbutane		33.50	38.30	39.90	37.00	33.50			40.00	0.98	2.20	-0.17
Isopentane		33.00	37.60	39.80	38.40	33.40	24.80		39.90	1.01	2.17	-0.17
2,2-Dimethylpropane			31.00	34.80	36.00	35.20	33.50	31.20	36.00	1.10	2.10	-0.15

Exponents α and β are calculated for ϕ at S_{max} according to [10] and [11].

Table 7: Burning velocities of unsaturated hydrocarbons and substituted alkyls at 25 C air-fuel temperature and 1 atm (0.31 mole % H_2O in air) [28]

	Equivalence Ratio ϕ								S_u in cm/s		T and P Exponents	
Chemical	0.7	0.8	0.9	1.0	1.1	1.2	1.3	1.4	S_{max}	ϕ at S_{max}	α	β
Acetylene		107.00 107.00	130.00	144.00 136.00	151.00	154.00 151.00	154.00	152.00 155.00	155.00	1.25	1.98	-0.12
Ethylene	37.00 37.00	50.00 48.00	60.00 60.00	68.00 66.00	73.00 70.00	72.00 72.00	66.50 71.00	60.00 65.00	73.50	1.13	2.08	-0.14
Propylene		62.00	66.60	70.20	72.20	71.20	61.00		72.50	1.14	2.07	-0.14
1,3-Butadiene			42.60	49.60	55.00	57.00	56.90	55.40	57.20	1.23	2.00	-0.12
n-1-Heptene		46.80	50.70	52.30	50.90	47.40	41.60		52.30	1.00	2.18	-0.17
Propylene			48.40	51.20	49.90	46.40	40.80		51.20	1.00	2.18	-0.17
n-2-Pentene		35.10	42.60	47.80	46.90	42.60	34.90		48.00	1.03	2.16	-0.16
2,2,4-Trimethyl-3-pentene		34.60	41.30	42.20	37.40	33.00			42.50	0.98	2.20	-0.17
Methanol		34.50	42.00	48.00	50.20	47.50	44.40	42.20	50.40	1.08	2.12	-0.15
Isopropyl alcohol		34.40	39.20	41.30	40.60	38.20	36.00	34.20	41.40	1.04	2.15	-0.16
Triethylamine		32.50	36.70	38.50	38.70	36.20	28.60		38.80	1.06	2.13	-0.16
n- Butyl chloride	24.00	30.70	33.80	34.50	32.50	26.90	20.00		34.50	1.00	2.18	-0.17
Allyl chloride	30.60	33.00	33.70	32.40	29.60				33.80	0.89	2.27	-0.19
Isopropyl mercaptan		30.00	33.50	33.00	26.60				33.80	0.94	2.23	-0.18
Ethylamine		28.70	31.40	32.40	31.80	29.40	25.30		32.40	1.00	2.18	-0.17
Isopropylamine		27.00	29.50	30.60	29.80	27.70			30.60	1.01	2.17	-0.17
n- Propyl chloride		24.70	28.30	27.50	24.10				28.50	0.93	2.24	-0.19
Isopropyl chloride		24.80	27.00	27.40	25.30				27.60	0.97	2.20	-0.18

Exponents α and β are calculated for ϕ at S_{max} according to [10] and [11].

Table 8: Burning velocities of aromatic compounds and cyclic Compounds at 25 C air-fuel temperature and 1 atm (0.31 mole % H_2O in air) [28]

	Equivalence Ratio ϕ								S_u in cm/s		T and P Exponents	
Chemical	0.7	0.8	0.9	1.0	1.1	1.2	1.3	1.4	S_{max}	ϕ at S_{max}	α	β
Furan	48.00	55.00	60.00	62.50	62.40	60.00			62.90	1.05	2.14	-0.16
Benzene		39.40	45.60	47.60	44.80	40.20	35.60		47.60	1.00	2.18	-0.17
Thiophene	33.80	37.40	40.60	43.00	42.20	37.20	24.60		43.20	1.03	2.16	-0.16
Ethylene oxide	57.20	70.70	83.00	88.80	89.50	87.20	81.00	73.00	89.50	1.07	2.12	-0.15
Butadiene monoxide		6.60	47.40	57.80	64.00	66.90	66.80	64.50	67.10	1.24	1.99	-0.12
Propylene oxide	41.60	53.30	62.60	66.50	66.40	62.50	53.80		67.00	1.05	2.14	-0.16
Dihydropyran	39.00	45.70	51.00	54.50	55.60	52.60	44.30	32.00	55.70	1.08	2.12	-0.15
Cyclopropane		40.60	49.00	54.20	55.60	53.50	44.00		55.60	1.10	2.10	-0.15
Tetrahydropyran	44.80	51.00	53.60	51.50	42.30				53.70	0.93	2.24	-0.19
Tetrahydrofuran			43.20	48.00	50.80	51.60	49.20	44.00	51.60	1.19	2.03	-0.13
Cyclopendadiene	36.00	41.80	45.70	47.20	45.50	40.60	32.00		47.20	1.00	2.18	-0.17
Ethylenimine		37.60	43.40	46.00	45.80	43.40	38.90		46.40	1.04	2.15	-0.16
Cyclopentane	31.00	38.40	43.20	45.30	44.60	41.00	34.00		45.40	1.03	2.16	-0.16
Cyclohexane			41.30	43.50	43.90	38.00			44.00	1.08	2.12	-0.15

Exponents α and β are calculated for ϕ at S_{max} according to [10] and [11].

Table 9: Burning velocities of selected silanes, aldehydes, ketones, esters, ethers, peroxides, and inorganics at 25 C air-fuel temperature and 1 atm (0.31 mole % H_2O in air) [28]

	Equivalence Ratio ϕ								S_u in cm/s		T and P Exponents	
Chemical	0.7	0.8	0.9	1.0	1.1	1.2	1.3	1.4	S_{max}	ϕ at S_{max}	α	β
Tetramethylsilane	39.50	49.50	57.30	58.20	57.70	54.50	47.50		58.20	1.01	2.17	-0.17
Trimethylethoxysilane	34.70	41.00	47.40	50.30	46.50	41.00	35.00		50.30	1.00	2.18	-0.17
Acrolein	47.00	58.00	66.60	65.90	56.50				67.20	0.95	2.22	-0.18
Propionaldehyde		37.50	44.30	49.00	49.50	46.00	41.60	37.20	50.00	1.06	2.13	-0.16
Acetaldehyde		26.60	35.00	41.40	41.40	36.00	30.00		42.20	1.05	2.14	-0.16
Acetone		40.40	44.20	42.60	38.20				44.40	0.93	2.24	-0.19
Methyl ethyl ketone		36.00	42.00	43.30	41.50	37.70	33.20		43.40	0.99	2.19	-0.17
Vinyl acetate	29.00	36.60	39.80	41.40	42.10	41.60	35.20		42.20	1.13	2.08	-0.14
Ethyl acetate		30.70	35.20	37.00	35.60	30.00			37.00	1.00	2.18	-0.17
Dimethyl ether		44.80	47.60	48.40	47.50	45.40	42.60		48.60	0.99	2.19	-0.17
Diethyl ether	30.60	37.00	43.40	48.00	47.60	40.40	32.00		48.20	1.05	2.14	-0.16
Dimethoxymethane	32.50	38.20	43.20	46.60	48.00	46.60	43.30		48.00	1.10	2.10	-0.15
Diisopropyl ether		30.70	35.50	38.30	38.60	36.00	31.20		38.90	1.06	2.13	-0.16
Dimethyl sulfide		29.90	31.90	33.00	30.10	24.80			33.00	1.00	2.18	-0.17
Di-tert -butyl peroxide		41.00	46.80	50.00	49.60	46.50	42.00	35.50	50.40	1.04	2.15	-0.16
Hydrogen	102.00 124.00	120.00 150.00	145.00 187.00	170.00 210.00	204.00 230.00	245.00 245.00	213.00	290.00	325.00	1.80	1.54	0.01
Carbon disulfide	50.60	58.00	59.40	58.80	57.00	55.00	52.80	51.60	59.40	0.91	2.25	-0.19
Carbon monoxide					28.50	32.00	34.80	38.00	52.00	2.05	1.34	0.06
Hydrogen sulfide	34.80	39.20	40.90	39.10	32.30				40.90	0.90	2.26	-0.19

Exponents α and β are calculated for ϕ at S_{max} according to [10] and [11].

Table 10: Burning velocities of various fuels at 100 C air-fuel temperature and 1 atm (0.31 mole % H_2O in air) [28]

	Equivalence Ratio ϕ								S_u in cm/s		T and P Exponents	
Chemical	0.7	0.8	0.9	1.0	1.1	1.2	1.3	1.4	S_{max}	ϕ at S_{max}	α	β
Propargyl alcohol		76.80	100.00	110.00	110.50	108.80	105.00	85.00	110.50	1.08	2.12	-0.15
Propylene oxide	74.00	86.20	93.00	96.60	97.80	94.00	84.00	71.50	97.90	1.09	2.11	-0.15
Hydrazine *	87.30	90.50	93.20	94.30	93.00	90.70	87.40	83.70	94.40	0.98	2.20	-0.17
Furfural	62.00	73.00	83.30	87.00	87.00	84.00	77.00	65.50	87.30	1.05	2.14	-0.16
Ethyl nitrate	70.20	77.30	84.00	86.40	83.00	72.30			86.40	1.00	2.18	-0.17
Butadiene monoxide	51.40	57.00	64.50	73.00	79.30	81.00	80.40	76.70	81.10	1.23	2.00	-0.12
Carbon disulfide	64.00	72.50	76.80	78.40	75.50	71.00	66.00	62.20	78.40	1.00	2.18	-0.17
n -Butyl ether		67.00	72.60	70.30	65.00				72.70	0.91	2.25	-0.19
Methanol	50.00	58.50	66.90	71.20	72.00	66.40	58.00	48.80	72.20	1.08	2.12	-0.15
Diethyl cellosolve	49.50	56.00	63.00	69.00	69.70	65.20			70.40	1.05	2.14	-0.16
Cyclohexan monoxide	54.50	59.00	63.50	67.70	70.00	64.00			70.00	1.10	2.10	-0.15
Epichlorohydrin	53.00	59.50	65.00	68.60	70.00	66.00	58.20		70.00	1.10	2.10	-0.15
n-Pentane		50.00	55.00	61.00	62.00	57.00	49.30	42.40	62.90	1.05	2.14	-0.16
n -Propyl alcohol	49.00	56.60	62.00	64.60	63.00	50.00	37.40		64.80	1.03	2.16	-0.16
n-Heptane	41.50	50.00	58.50	63.80	59.50	53.80	46.20	38.80	63.80	1.00	2.18	-0.17
Ethyl nitrite	54.00	58.80	62.60	63.50	59.00	49.50	42.00	36.70	63.50	1.00	2.18	-0.17
Pinene	48.50	58.30	62.50	62.10	56.60	50.00			63.00	0.95	2.22	-0.18
Nitroethane	51.50	57.80	61.40	57.20	46.00	28.00			61.40	0.92	2.24	-0.19
Iso-octane		50.20	56.80	57.80	53.30	50.50			58.20	0.98	2.20	-0.17
Pyrrole		52.00	55.60	56.60	56.10	52.80	48.00	43.10	56.70	1.00	2.18	-0.17
Aniline		41.50	45.40	46.60	42.90	37.70	32.00		46.80	0.98	2.20	-0.17
Dimethyl formamide		40.00	43.60	45.80	45.50	40.70	36.70		46.10	1.04	2.15	-0.16

Exponents α and β are calculated for ϕ at S_{max} according to [10] and [11].

A Ignition Potential of Gases and Dusts

Effective energy levels and semi-quantitative rates of heating of typical ignition sources are shown in Figure 16 and 17. Electrical sparks can be caused by short circuits, electric arcs, contact resistance, electrostatic charge, static electricity, lightening discharge, etc. A car spark plug can generate 25 mJ of ignition energy while cleaning of shoes at a doormat can result in 22 mJ of static electricity.

Figure 16: Typical ignition sources rates of heating

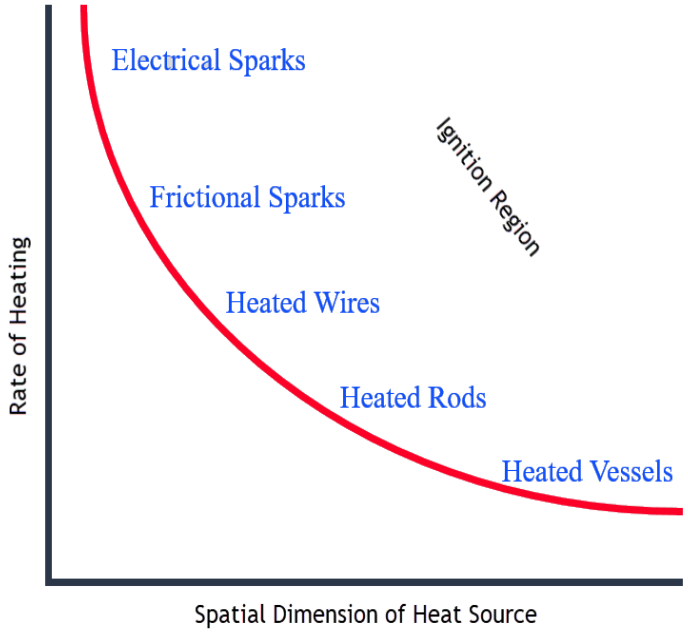

Minimum ignition energy (MIE) is defined as the smallest amount of energy needed to cause a flame to propagate for a given system. Measured MIE values are apparatus dependent and are influenced by:

- the rate of energy deposition,
- the method of heat addition, and
- the geometry of the heating source.

Large rates of energy deposited into a flammable medium over very short durations can lead to direct initiation of detonation. What is typically done in experimental determination of MIE values is to reduce the energy deposition rate until flame propagation stops. A capacitor discharge spark is found to yield the lowest MIE for flammable gas and/or combustible dust mixtures. High performance condensers are usually used in experimental setups so that maximum energy is discharged through the spark gap. The amount of stored energy is [4]:

$$E = \frac{CV^2}{2} \tag{37}$$

[4] $V = I\ R$ where I is current in Amps and R is resistance in Ohms

Figure 17: Effective energy levels, materials at risk of ignition, and types of ignition sources [29]

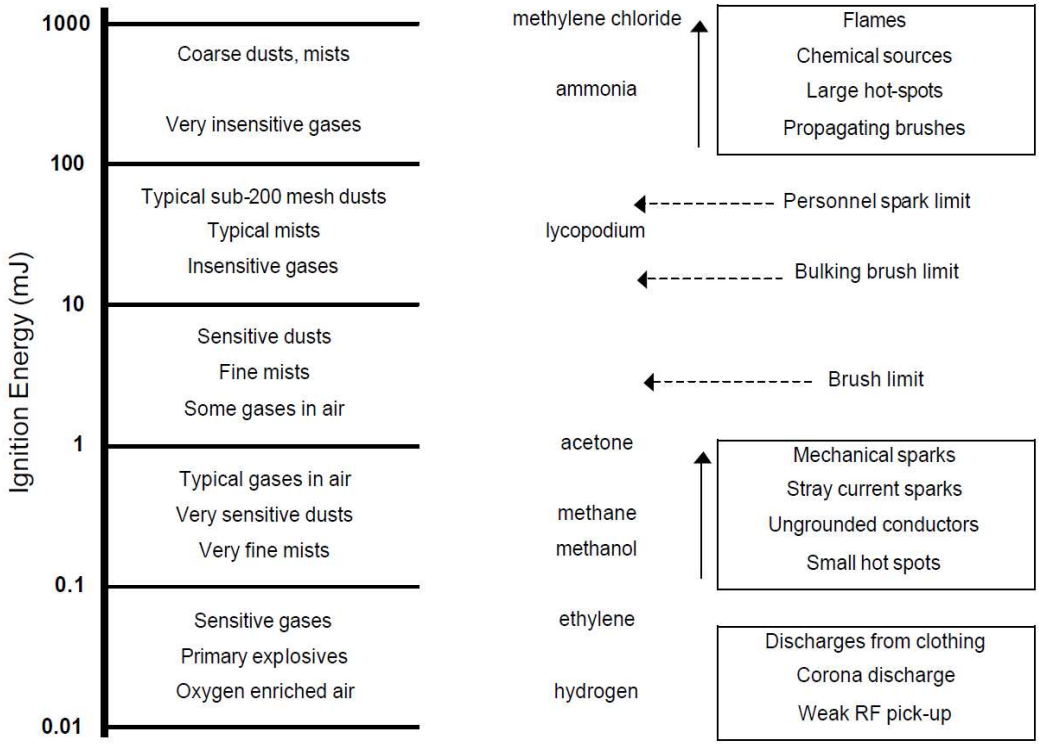

where, C is the capacitance in Farads and V is the voltage in Volts. A small fraction of the stored energy is lost due to conduction to the electrodes. Total energy can be modified by changing C and/or V. Electrode spacing is changed as an independent parameter to assess its impact on the value of MIE. If the spacing is too small, interaction between the flame and the electrode causes the MIE to increase (see Figure 20). If the gap is too large, the flame area increases because the source geometry becomes cylindrical. This also yields an increase in the value of MIE.

A.1 Minimum Ignition Energy for Gases

It has been shown that MIE [30] is proportional to the ratio of thermal conductivity over laminar burning velocity:

$$\text{MIE} \quad = \quad \pi d^2 \frac{k}{s_u} \left[T_f - T_u\right] \tag{38}$$

where d is the quenching distance, k is the thermal conductivity, s_u is the laminar burning velocity, T_f is the flame temperature, and T_u is the starting gas temperature. Equation 38 predicts best at high temperatures and fast burning since the equation only considers thermal energy transport and ignores chemical energy transport by internal diffusion of reactants and products. If we carefully examine Equation 38, it indicates that MIE should occur at the point of maximum burning. Maximum laminar burning velocity usually occurs at near stoichiometric fuel-air compositions for most hydrocarbon-air systems. Figure 18 shows that the point of minimum MIE occurs near stoichiometric for methane-air and shifts towards the rich side for higher order hydrocarbons. This is

mainly due to the preferential diffusion of oxygen into the reaction zone which shifts the composition towards stoichiometric.

Equation 38 indicates that higher temperatures should yield lower MIE. As T_u increases the burning velocity increases and the quenching distance decreases. The minimum ignition energy and quenching distance decrease with increasing pressures for most hydrocarbon-air systems.

Figure 18: Minimum ignition energies vs. stoichiometry for various fuel-air mixtures [30]

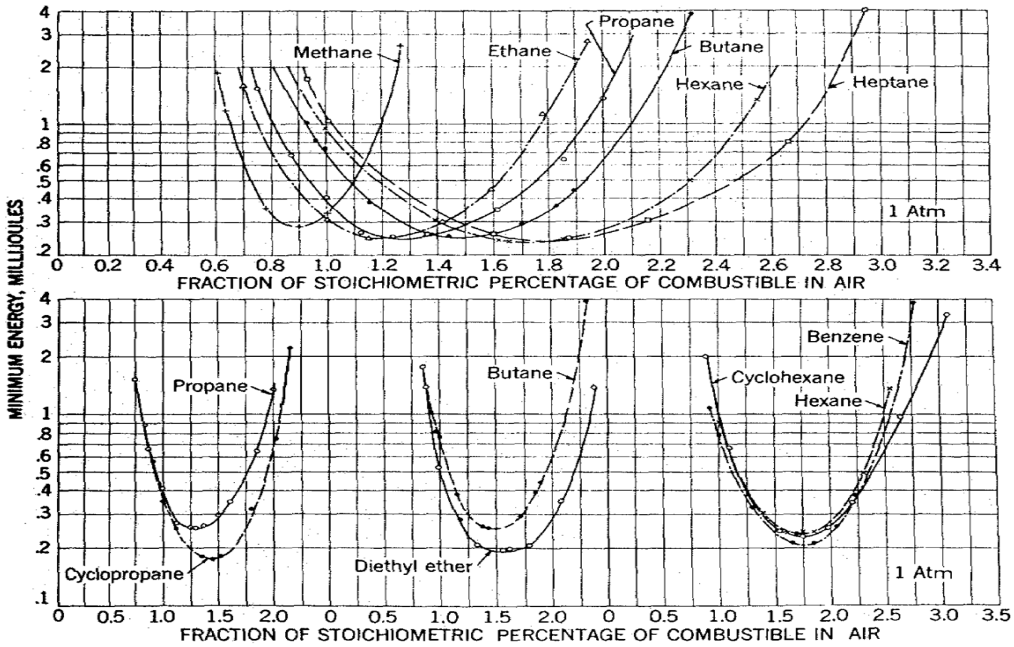

A.2 Minimum Ignition Energies for Dusts

In addition to ignition source geometry and rate, MIE values for dusts depend on other factors such:

- particle size,
- turbulence,
- moisture/volatiles content, and
- dust composition / hybrid mixtures.

Small particles possess a larger surface to volume ratio than larger particles. While particle size does not really affect the theoretical maximum pressure attained in a closed volume with rigid walls, it has a pronounced effect on ease of ignition and propagation of flames. Smaller particles require lower ignition energies and lead to larger pressure rise rates.

Once ignition is achieved, turbulence leads to flame acceleration and subsequently higher pressure rise rates.

The presence of moisture in dust particles affects the autoignition temperature. The autoigtion temperature of moist particles is higher than that of dry particles. Thus MIE values obtained for moist particles are higher than values reported for dry particles.

Experimentally determined values of MIE's depend on many factors as outlined in the previous section. Spark ignition has been shown to yield the lowest MIE values for dusts and flammable gas mixtures. Minimum values are obtained by varying the capacitance and voltage at fixed electrode gaps. The electrode gap is then reduced until the quenching distance is reached.

It is recommended that MIE values used for safe equipment design should be obtained consistently for all applications. For example, adopting a method such as the one outlined by Dahn et al. [31] may provide a standardized method for MIE evaluation. However, effects of energy deposition durations on MIE values need to be better quantified.

Table 11 provides some general guidance on ignition potential of dusts and hybrid mixtures. The probability of ignition depends on both product properties (sensitivity) and the process type and conditions (ignition intensity). Experience shows that in well designed plants, with only conducting parts, which are well grounded and bonded, with no internally coated surfaces, explosions due to electrostatics only seem to occur with products with an MIE less than 10 mJ.

With carbon and stainless steel materials of construction, the following rule can be used: if MIE $<$ 100 mJ or MIT $<$ 400 C, then ignition is possible.

Table 11: General dust and hybrid system ignition potential guidance [27]

MIE	**Ignition Source**	**Ignition Probability**
MIE $<$ 4 mJ	Almost all ignition sources, including brush discharges	Imminent
4 $<$ MIE $<$ 10 mJ	Most ignition sources (brush discharges probably not)	Very probable
10 $<$MIE $<$ 100 mJ	Some electrostatic discharges	Less probable
100 $<$ MIE $<$1000 mJ	Only very intensive electrostatic discharges	Not probable
MIE $>$ 1000 mJ	Only extremely intensive electrostatic discharges (lightning)	Not expected

A.3 Ignition Delay and Autoignition

Consider a flammable mixture which is heated to a high enough temperature such that ignition will occur due to large reaction rates. The time delay before ignition or the time lag before ignition is defined as the time elapsed from the instant the mixture temperature is raised until the instant a flame is observed. At high temperatures, the time delay for any particular configuration can be represented by the following relation [32]:

$$\ln\left[\tau X_F^n X_O^m\right] = \frac{E}{RT} + B \tag{39}$$

where, E is the activation energy in $\mathrm{cal/gmol}$, and B, n, and m are constants. Figure 19 shows how ignition delay varies with temperature. Increasing temperatures result in higher reaction rates

and lower delay times. Decreasing temperatures result in slower reaction rates and longer ignition delay times. There is a limit beyond which ignition will not occur. This limit is often referred to as the autoignition temperature or the spontaneous ignition temperature. This is the lowest temperature at which ignition will occur. The autoignition temperature is apparatus dependent and is usually measured in uniformly heated vessels which are large enough so that quenching effects are minimized.

Figure 19: Time delay before ignition of n-propyl nitrate in air at 1000 psig from 150 to 170 C [32]

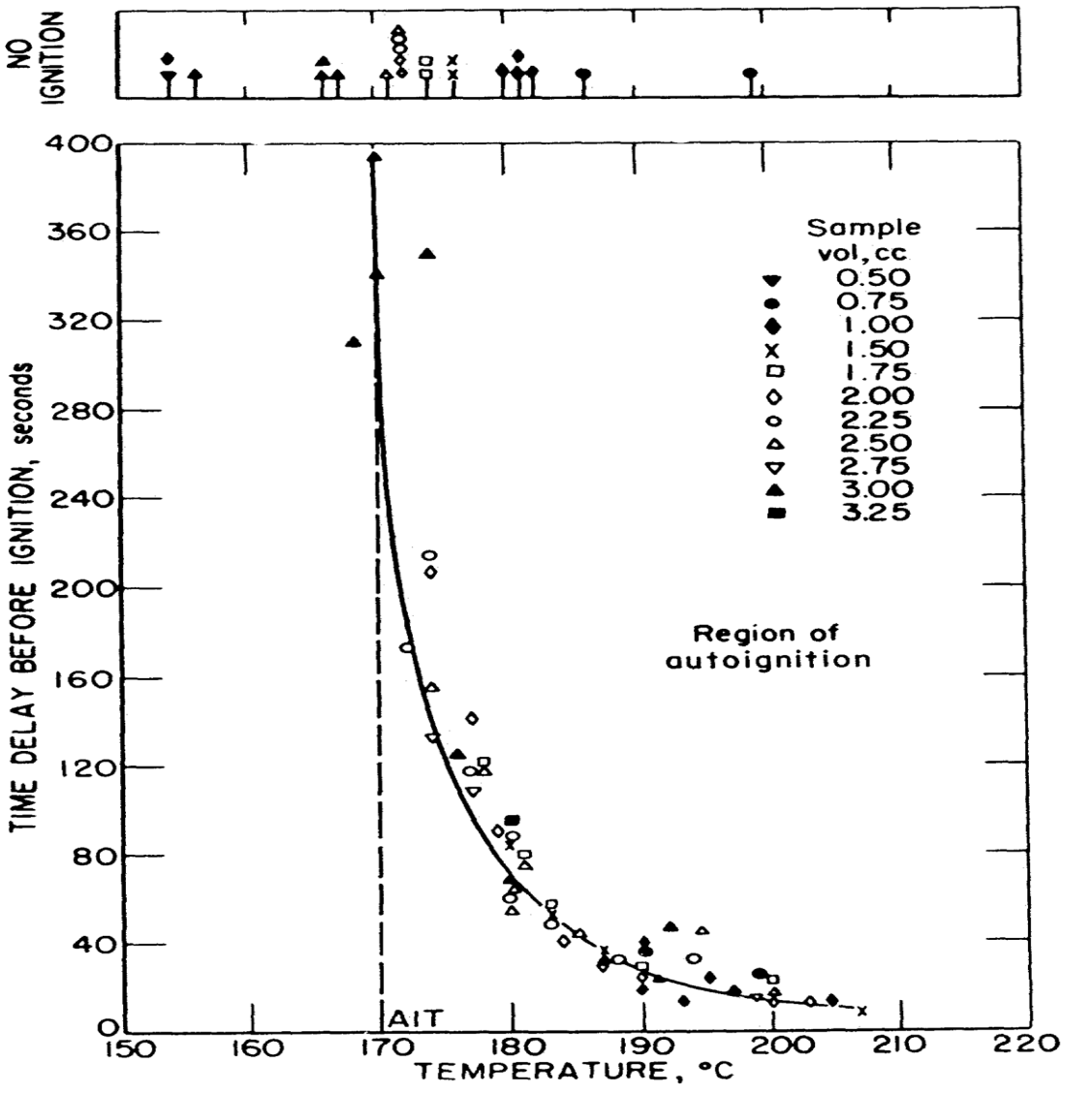

A.4 Quenching Distance

Quenching distance is defined as the largest channel dimension that will just keep a flame from propagating throughout the channel. If the channel dimensions are small enough, enough heat is lost by the flame as it passes through the channel and the flame is quenched. The quenching distance is determined experimentally by causing ignition to a flammable gas/dust mixture using a

pair of flanged (parallel plates) electrodes. If the mixture is ignitable in the presence of the plates, the gap between the plates is reduced until the quenching distance is reached.

The quenching distance for flat plates is about 65 % of that measured using circular tubes. The quenching distance varies as a function of the inverse of pressure. It is also related to minimum ignition energy. Figure 20 shows that MIE depends on the square of the quenching distance for most hydrocarbon air systems.

Figure 20: The relation between quenching distance and spark minimum ignition energies for a number of hydrocarbon-air mixtures [30]

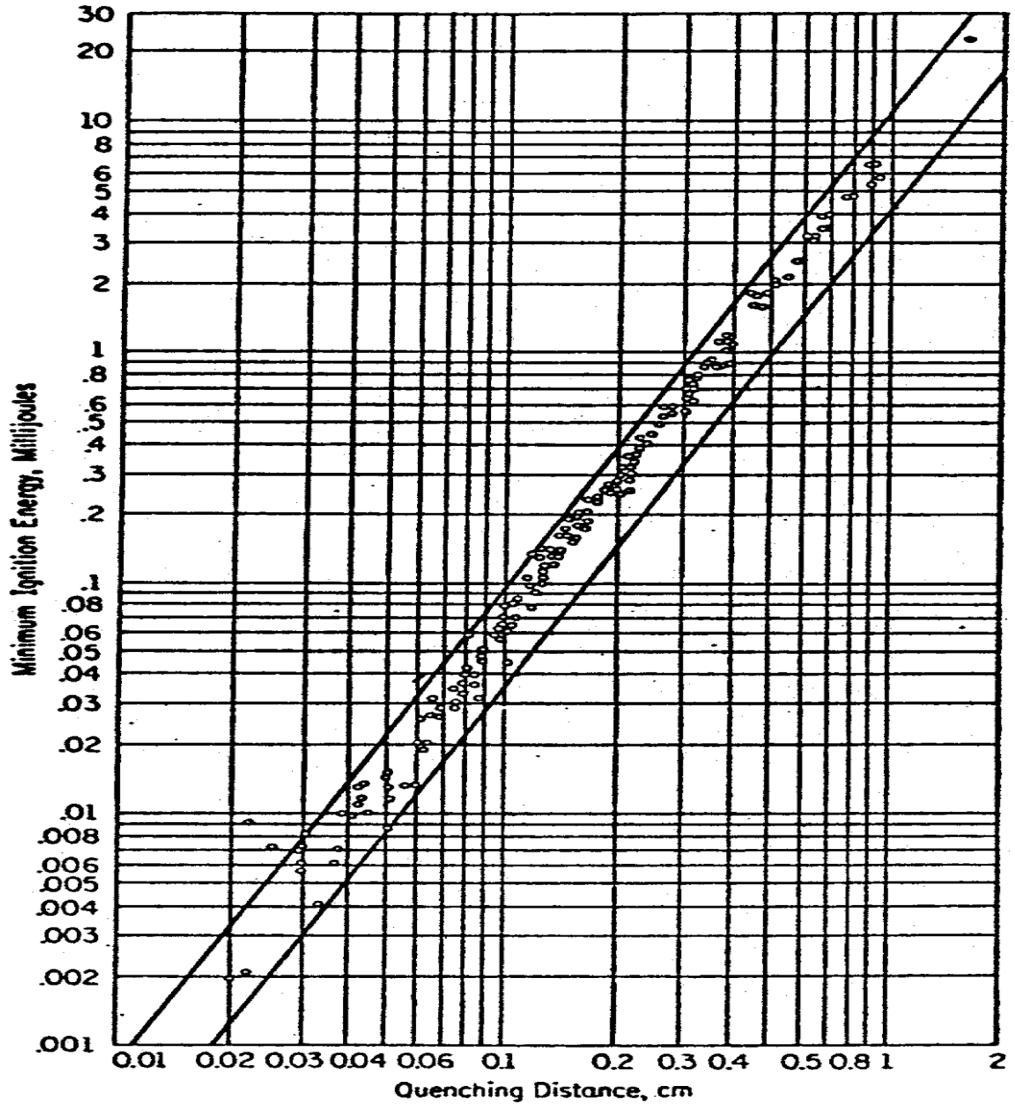

B Simplified Deflagration Venting Sizing Methods for Dusts

B.1 Venting for Low Pressure Structures

Enclosures with a maximum allowable overpressure of 0.1 bar are considered as low pressure structures. The ratio of required vent area to enclosure surface area is proportional to the inverse of the square root of the maximum overpressure that can be withstood by the weakest structural element:

$$\frac{A_h}{A_{st}} = C\frac{1}{\sqrt{P_f}} \tag{40}$$

where P_f is the maximum overpressure developed during a vented deflagration, A_h is the vent area, and $A_{st}$is the total vessel surface area. NFPA 68 [33] reports values of C of 0.26, 0.3, and 0.51 $\mathrm{kPa}^{1/2}$ for St-1, St-2 and St-3 dusts respectively.

A more detailed version of Equation 40 was presented by Swift and Epstein [34]:

$$\frac{A_h}{A_{st}} = \frac{\chi s_u \rho_u}{C_d G\sqrt{\frac{P_f}{P_0}-1}}\left[\left(\frac{P_{\max}}{P_0}\right)^{1/\gamma_b} - 1\right] \tag{41}$$

χ is a turbulence enhancement factor, s_u is the laminar burning velocity, C_d is the vent discharge coefficient, ρ_u is the unburnt material density, G is the vented material mass flux, $P_{\max}$ is the maximum closed (without venting) vessel absolute pressure, P_0 is the initial absolute pressure prior to ignition, γ_b is the heat capacity ratio for combustion products, and P_f is the maximum absolute pressure developed during a vented deflagration

B.2 Venting for High Pressure Structures

We consider high pressure enclosures with allowable overpressure of 0.1 bara or more as high pressure structures. Palmer [35] presents the following equation for the estimation of overpressure for high-pressure structures:

$$\frac{P - P_s}{P_s} = 2.30\frac{\rho_c}{C_d^2\gamma^2}\left[\frac{V}{A}\frac{1}{P_{\max}^{3/2}}\left(\frac{dP}{dt}\right)_{\max}\right]^2 \tag{42}$$

where, P is the maximum pressure developed in the vessel/enclosure, P_s is the starting initial pressure, and ρ_c is the density of unburnt dust in suspension.

In Equation 42 $\frac{dP}{dt}$ can be substituted for by:

$$\left[\frac{dP}{dt}\right]_{\max} = \frac{K_{st}}{V^{1/3}} \tag{43}$$

Algebraic manipulations of Equation 42 leads to the following expression for vent area:

$$A_h = a\left[P - P_s\right]^{-1/2} V^{2/3} K_{st} \tag{44}$$

where a is a constant given by:

$$a = \frac{1}{P_{\max}^{3/2}}\left[2.30\frac{\rho_c}{C_d^2\gamma^2}\right]^{1/2} \tag{45}$$

NFPA 68 [33] published a similar formula for explosion venting in its guidelines for venting. The formula is based on comprehensive explosion tests of four dusts in reference [36]:

$$A_h = aV^{2/3}K_{st}^b P_{\text{red}}^c \tag{46}$$

where, a, b, and c are constants given by the following equations:

$$a = 0.000571 \exp\left(2P_{\text{stat}}\right) \tag{47}$$
$$b = 0.978 \exp\left(-0.105P_{\text{stat}}\right) \tag{48}$$
$$c = -0.687 \exp\left(0.226P_{\text{stat}}\right) \tag{49}$$

P_{red} is the maximum pressure developed during venting in barg and P_{stat} is the vent relief pressure in barg. The formulas are applicable for $50 \leq K_{st} < 600$, $0.2 \leq P_{\text{red}} < 2$ and $0.1 \leq P_{\text{stat}} < 0.5$.

NFPA 68 also presents similar equations for flammable gas.

$$A_h = dV^{f+2/3} \exp(gP_{\text{stat}}) P_{\text{red}}^h \tag{50}$$

where the constants d, f, g and h are shown in Table 12.

Table 12: Constants for use in NFPA 68 [33] gas explosion venting nomograph

Gas	d	f	g	h
Methane	0.105	0.104	1.230	-0.823
Propane	0.148	0.037	0.942	-0.671
Coke Gas	0.150	0.029	1.380	-0.707
Hydrogen	0.279	0.014	0.755	-0.393

These equations were also presented as graphs in NFPA 68 [33] such as the one shown in Figure 21 for methane.

Special consideration must be given to enclosures designed with large L/D venting ducts where flame acceleration is important and may lead to more severe and localized damage. Ducting used in conjunction with venting should be maintained as short as possible.

For pressure relief through doors, it is important to note that the use of hinges may create negative pressures following an explosion which can lead to implosion of containment. This is mainly caused by the potential of the door swinging closed. Other issues to be considered include the total weight of door assemblies. For example, NFPA guidelines for venting recommend that the door weight should be kept as low as possible and should not exceed 2.5 lb/ft^2 in any case.

In order to reduce knock-on effects, Process units equipped with explosion relief vents should be sited away from the facility whenever possible.

Figure 21: NFPA 68 [33] venting nomograph for methane. P_{red} is maximum pressure developed during venting and P_{stat} is vent closure release pressure

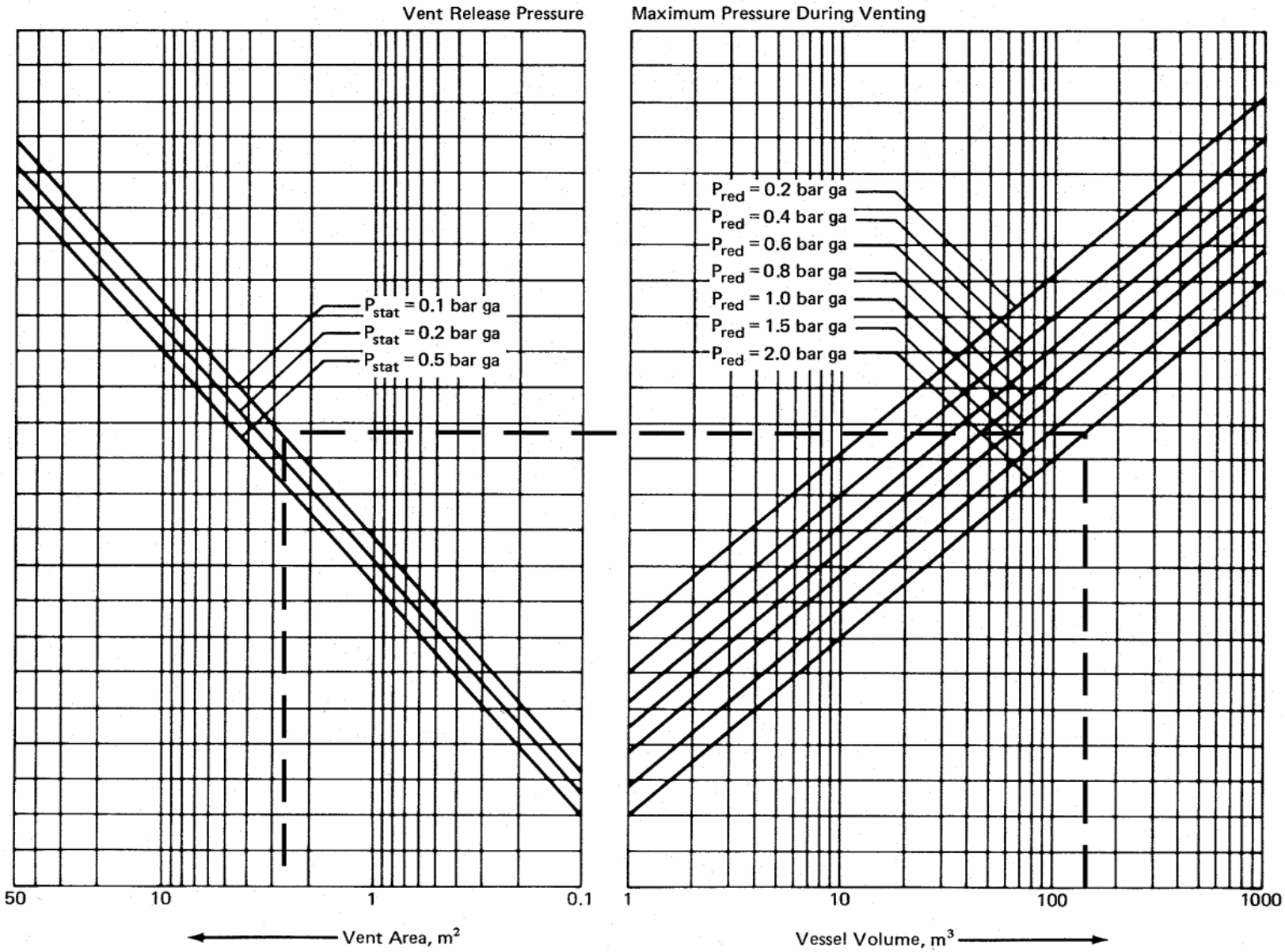

Figure 6-2(a) Venting Nomograph for Methane.

C Simplified Deflagration Venting Sizing Methods for Gases

C.1 NFPA 68

Equation 40 is also used in the 2018 edition of NFPA 68 [1] for the calculation of deflagration venting requirements of gas mixtures and mists in enclosures with short vent lines ($L/D \leq 5$):

$$\frac{A_h}{A_{st}} = C\frac{1}{\sqrt{P_f}} \tag{51}$$

where P_f (≤ 0.5 barg) is the maximum pressure developed during a vented deflagration, A_h is the vent area, and A_{st} is the total vessel surface area. C is defined as:

$$C = \frac{\chi s_u \rho_u}{2C_d G}\left[\left(\frac{P_{\max}+1}{P_0+1}\right)^{1/\gamma_b} - 1\right]\sqrt{P_0+1} \tag{52}$$

χ is a turbulence enhancement factor, s_u is the laminar burning velocity, C_d is the vent discharge coefficient, ρ_u is the unburnt material density, G is the vented material mass flux, $P_{\max}$ is the maximum closed (without venting) vessel pressure, P_0 is the initial pressure prior to ignition, and γ_b is the heat capacity ratio for combustion products.

C.2 The Method of Bradley and Mitcheson

The NFPA 68 [33] equations for gases and dusts do not allow for the estimation of relief requirements for deflagrations in vessels or enclosures where the set pressure is higher than 2 barg or where the maximum allowable pressure is higher than 2 barg.

Bradley and Mitcheson [6, 7] provided two simple expressions for the estimation of relief requirement for gas explosions (deflagrations) in vessels. These expressions are based on available experimental data and theoretical predictions of a mathematical model developed by Bradley and Mitcheson.

Relief requirements estimated using the Bradley and Mitcheson expressions are conservative. They do not apply to vessels with long vent lines, i.e. $L/D > 20$.

Using the Bradley and Mitcheson expressions we can estimate the value of required relief for initially open vents and initially closed vents.

For an initially open vent:

$$A_h \geq \left(\frac{A_{st}}{C_d}\right)(\chi \overline{s}_{u_o}) \exp\left[\frac{0.64 - \Delta P_m}{2}\right] \text{ for } \Delta P_m \geq 1 \text{ atm} \tag{53}$$

$$A_h \geq \left(\frac{A_{st}}{C_d}\right)(\chi \overline{s}_{u_o}) \sqrt{\left[\frac{0.7}{\Delta P_m}\right]} \text{ for } \Delta P_m < 1 \text{ atm} \tag{54}$$

$$\Delta P_m = P_m - P_s \tag{55}$$

For an initially closed vent:

$$A_h \geq \left(\frac{A_{st}}{C_d}\right)(\chi \overline{s}_{u_o}) \left[\frac{2.4}{P_{open} - 1}\right]^{1.43} \text{ for } P_{open} \geq 2 \text{ atm} \tag{56}$$

$$A_h \geq \left(\frac{A_{st}}{C_d}\right)(\chi \overline{s}_{u_o}) \sqrt{\left[\frac{12.3}{P_{open} - 1}\right]} \text{ for } P_{open} < 2 \text{ atm} \tag{57}$$

A_h is the required vent area, A_{st} is the vessel surface area, C_d is a discharge coefficient, P_m is the maximum pressure reached in the vessel in atm, P_s is the starting initial pressure or ambient pressure in atmospheres, P_{open} is the vent opening pressure in atm, and χ is a turbulence factor which accounts for the increase in burning velocity due to initial mixture turbulence or the presence of obstacles.

The expressions outlined in Equations 56 and 57 assume that the maximum pressure reached in the vessel/enclosure is equal to the vent opening pressure.

$\overline{s}_{u_o}$ is a normalized burning velocity, defined by Bradley and Mitcheson as:

$$\overline{s}_{u_o} = \left(\frac{s_{u_o}}{c_0}\right)\left(\frac{\rho_{u0}}{\rho_{b0}} - 1\right) \tag{58}$$

$$c_0 = \sqrt{\gamma_u \frac{R_g}{M_{w_u}} T_0} \tag{59}$$

s_{u_o} is the laminar burning velocity, c_0 is the speed of sound in the unburnt gas at initial temperature and pressure, ρ_{u0} is the density of the unburnt gas at initial temperature and pressure, ρ_{b0} is the density of the combustion products at initial temperature and pressure, γ_u is the ratio of heat capacities for the unburnt gas, and M_{w_u} is the molecular weight of the unburnt gas. The value of χ can be estimated based on guidance provided earlier [13, 14].

The density ratio ρ_{u0}/ρ_{b0} is an expansion ratio due to combustion. For an ideal gas it is equal to:

$$\frac{\rho_u}{\rho_b} = \frac{T_f}{T_0}\frac{N_b}{N_u} \tag{60}$$

where N_b is the number of moles of gas combustion products produced per N_u moles of reactants. For hydrocarbon combustion reactions, $N_b \simeq N_u$ and the expansion ratio can be expressed as the temperature ratio. This is illustrated in Table 13 for many hydrocarbon gases and hydrogen. The expansion ratio ranges from 7 to 9 for most hydrocarbons ([37]).

For vessels having maximum allowable pressure or set pressure greater than 44 psig and where simplified methods are preferred, use the Bradley Mitcheson sizing method. For multi-product service or non-dedicated use, assume a solvent of burning velocity at least equivalent to that of methanol, i.e. ≥ 0.57 m/s. Assume the vessel to be 80 % full, discharge coefficient of 0.6 and pressure accumulation not to exceed 20 % of maximum allowable working pressure. Assume the turbulence factor, χ, to be at least 1.5 and the vent to be initially closed.

Figure 22: Detailed estimate of required deflagration venting using SuperChems Expert v3.1

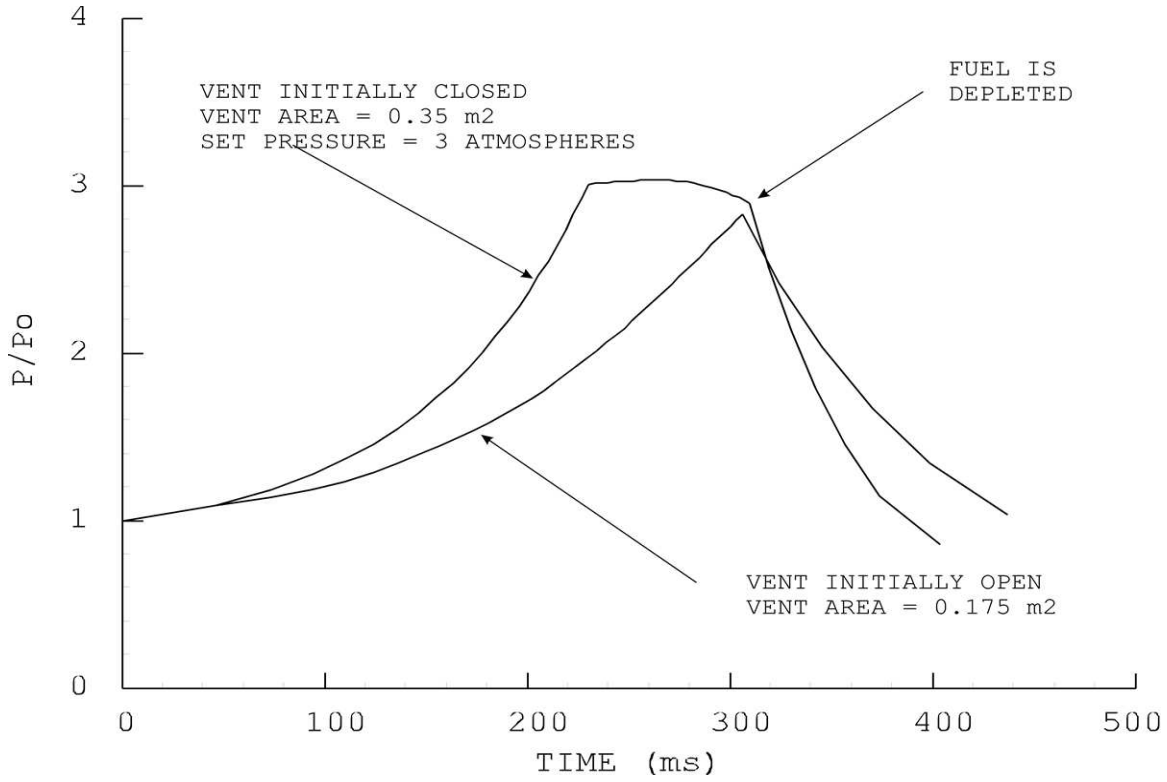

C.3 Example: Deflagration Vent Sizing; Vapor/Liquid System

A 1,000 gallon vessel, shown in Figure 23, is in agitated acetone storage service. It is assumed that internal vapor space ignition is the controlling relief scenario. What is the required rupture disk size ?

C.3.1 Required Data:

- Vessel design pressure (P_{des}): 100 psig
- Vessel diameter (D): 5 ft
- Vessel straight side length (L): 6 ft
- Molecular weight of acetone (M_w): 58.1
- Ratio of heat capacities (γ): 1.103
- Gas constant (R_g): 8,314 J/kmol/K
- Vapor temperature at onset of deflagration (T_0): 298 K
- Adiabatic flame temperature (T_f): 2,307 K
- Acetone laminar burning velocity (s_{u_o}): 0.423 m/s

Figure 23: Example: Deflagration Vent Sizing For a Vapor/Liquid System

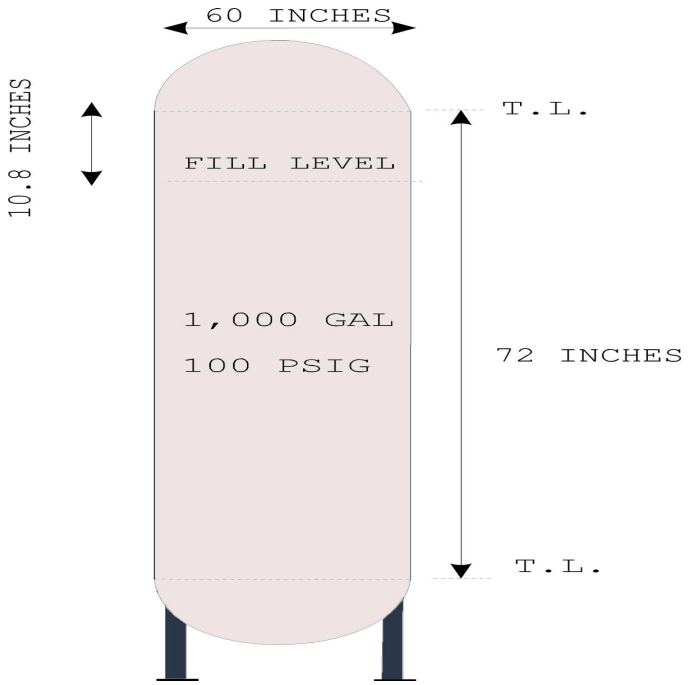

- Moles of combustion products produced per mole of reactants (N_b/N_u): 6/5 = 1.2
- Vent set pressure (P_{open}): 7.8 atmospheres or 100 psig

C.3.2 Assumptions:

- Pressure at onset of ignition (P_s): 14.7 psia
- Discharge coefficient (C_d): 0.6
- Turbulence factor, χ, of 1.5 since vessel is closed and does not contain objects and mixture is initially at rest.

C.3.3 Solution:

1. Determine maximum pressure:

$$\begin{aligned} P_m &= 1.2P_{des} + 14.7 \\ &= 1.2 \times 100 + 14.7 \\ &= 134.7 \text{ psia} \\ &= 9.16 \text{ atm} \end{aligned}$$

and

$$\begin{aligned} \Delta P_m &= P_m - P_s \\ &= 9.16 - 1 \\ &= 8.16 \text{ atm} \end{aligned}$$

2. Calculate unwetted internal surface area:

$$\begin{aligned} A_{st} &= A_{head} + A_{cylindrical} \text{ where} \\ A_{head} &= 1.38 \times \pi \times D^2/4 \\ &= 1.38 \times 3.14 \times (60/12)^2/4 \\ &= 27.08 \text{ ft}^2 \end{aligned}$$

To calculate $A_{cylidrical}$, first determine straight side dry dimension,

$$\begin{aligned} V_{tot} &= 1027 \text{ gal and at 80 \% full} \\ V_{80} &= 0.8 \times V_{tot} = 0.8 \times 1027 = 821.6 \text{ gal} \end{aligned}$$

Of this wetted volume, the straight section contains,

$$\begin{aligned} V_{stwet} &= V_{80} - V_{head} \\ &= 821.6 - 72.9 \text{ (ASME F \& D head)} \\ &= 748.7 \text{ gal or} 100.1 \text{ ft}^3 \end{aligned}$$

The wetted straight side height is,

$$\begin{aligned} L_{stwet} &= \text{Volume/Area} \\ &= 100/(3.14 \times 5^2/4) \\ &= 5.1 \text{ ft} \end{aligned}$$

The unwetted straight side length becomes,

$$\begin{aligned} L_{stdry} &= L - L_{stwet} \\ &= 6 - 5.1 \\ &= 0.9 \text{ ft} \end{aligned}$$

The unwetted cylindrical area becomes,

$$\begin{aligned} A_{cylindrical} &= \pi D L_{stdry} \\ &= 3.14 \times 5 \times 0.9 \\ &= 14.13 \text{ ft}^2 \end{aligned}$$

Finally,

$$\begin{aligned} A_{st} &= A_{head} + A_{cylindrical} \\ &= 27.08 + 14.13 \\ &= 41.21 \text{ ft}^2 \text{ or } 3.84 \text{ m}^2 \end{aligned}$$

3. Calculate the speed of sound in the unburnt gas medium:

$$\begin{aligned} c_0 &= \sqrt{\gamma \frac{R_g}{M_w} T_0} \\ &= \sqrt{1.103 \times \frac{8,314}{58.1} \times 298} \\ &= 216.9 \text{ m/s} \end{aligned}$$

4. Calculate the vapor expansion ratio:

$$\begin{aligned} \frac{\rho_u}{\rho_b} &= \frac{T_f}{T_0}\frac{N_b}{N_u} \\ &= \frac{2,307}{298}\frac{6}{5} \\ &= 9.29 \end{aligned}$$

5. Calculate the normalized burning velocity:

$$\begin{aligned} \overline{s}_{u_0} &= \frac{s_{u_o}}{c_0}\left(\frac{\rho_u}{\rho_b} - 1\right) \\ &= \frac{0.432}{216.9}(9.29 - 1) \\ &= 0.0165 \end{aligned}$$

6. Calculate the required rupture disk area: (with the vent initially closed, use Equation 6.16)

$$\begin{aligned} A_h &= \left(\frac{A_{st}}{C_d}\right)\left(\chi \overline{S}_0\right)\left[2.4/(P_{open} - 1)\right]^{0.143} \\ &= \left(\frac{3.84}{0.6}\right)(1.5 \times 0.0165)\left[2.4/(7.8 - 1)\right]^{0.143} \\ &= 0.1363 \text{ m}^2 \\ &= 211.6 \text{ in}^2 \text{ or } D = 16.4 \text{ in} \end{aligned}$$

C.4 Example: Deflagration Vent Sizing; All Gas Systems

Consider a spherical vessel which contains a stoichiometric mixture of methane and air at 298 K and 1 atmosphere. The vessel is 10 m^3 in volume and has a maximum allowable accumulation pressure limit of 3 atm. No turbulence is present prior to ignition. Using the Bradley-Mitcheson simple formulas, estimate the deflagration relief requirements for two cases:

1. Vent is initially closed and has a set pressure of 3 atm.
2. Vent is initially open at 1 atm.

Use a discharge coefficient of 0.6.

C.4.1 Solution

The following is a step by step procedure which illustrates the use of the Bradley-Mitcheson sizing formulas:

1. Calculate vessel surface area. Since the vessel is spherical, the total surface area can be calculated as $4\pi r^2$, where r is the vessel radius:

$$\begin{aligned} V &= 10 = \frac{4}{3}\pi r^3 \\ r &= \left(\frac{3\times 10}{4\times\pi}\right)^{1/3} = 1.3365 \text{ m} \\ A_{st} &= 4\pi r^2 = 22.56 \text{ m}^2 \end{aligned}$$

2. Calculate the speed of sound in the unburnt gas medium. This requires information on the molecular weight and heat capacities ratio of the mixture. According to Table 13, a methane-air mixture is stoichiometric at a mixture composition of 9.5 % methane, 19.01 % oxygen and 71.5 % nitrogen.

$$\begin{aligned} M_{w_u} &= 0.095\times 16 + 0.1901\times 32 + 0.715\times 28 = 27 \text{ kg/kmol} \\ \gamma_u &= 1.338 \text{ (From the JANAF tables)} \\ c_0 &= \sqrt{\gamma_u \frac{R_g}{M_{w_u}} T_0} = \sqrt{1.338\times\frac{8,314}{27}\times 298} = 352.7 \text{ m/s} \end{aligned}$$

3. Calculate the normalized burning velocity. The expansion ratio for methane-air is 7.4 and the laminar burning velocity, s_{u_o}, is 0.45 m/s (from Table 13).

$$\overline{s}_{u_0} = \left(\frac{s_{u_o}}{c_0}\right)\left(\frac{\rho_{u0}}{\rho_{b0}} - 1\right) = \left(\frac{0.45}{352.7}\right)(7.4-1) = 0.008165$$

4. Estimate the turbulence factor, χ. Since the vessel does not contain any obstacles and the mixture is initially at rest, we set χ to 1.5.

5. Estimate the required relief area for case 1, vent is initially closed. Since P_{open} is greater than 2 atmospheres,

$$A_h = \left(\frac{22.56}{0.6}\right)(1.5\times 0.008165)\left[\frac{2.4}{3-1}\right]^{1.43} = 0.615 \text{ m}^2$$

6. Estimate the required relief area for case 2, vent is initially open.

   (a) Calculate ΔP_m.

$$\Delta P_m = 3.0 - 1.0 = 2.0 \text{ atm}$$

   (b) Since ΔP_m is greater than 1 atm,

$$A_h = \left(\frac{22.56}{0.6}\right)(1.5\times 0.008165)\exp\left[\frac{0.64-2}{2}\right] = 0.233 \text{ m}^2$$

Figure 22 illustrates the use of SuperChems Expert v3.1 to estimate the required deflagration relief for cases 1 and 2. The detailed estimates are 0.35 m^2 and 0.175 m^2 for cases 1 and 2. The Bradley-Mitcheson estimates, are 0.615 m^2 and 0.233 m^2 respectively.

C.5 Reduced Set Points

The Bradley-Mitcheson equations (see Section C.2), in their original form, do not accommodate the use of significant overpressure, or effectively, a lowered relief device set point. A lowered set point should allow for a reduced relief vent area requirement.

An alternative approach uses a modification proposed by Epstein et al. [14]. The method provides for the use of a set point for pressures higher than 15 psig. Epstein et al. derive the following closed form solution for peak pressure at the end of combustion:

$$\frac{P_f}{P_0} = \frac{P_{max}}{P_0}\left[\frac{\lambda + B}{1 + B}\right]^{\gamma_b} \tag{61}$$

where P_f is the peak pressure at end of combustion, P_0 is the pressure prior to ignition, γ_b is the heat capacity ratio of the combustion products, B is the ratio of maximum burn rate to sonic discharge rate, and λ is a dimensionless vent opening pressure ratio. B and λ are defined by the following equations:

$$B = \frac{\chi s_{u_o} \rho_u A_{st}}{G C_d A_h} \tag{62}$$

$$\lambda = \frac{\left(\frac{P_{set}}{P_0}\right)^{(1/\gamma_b)} - 1}{\left(\frac{P_{max}}{P_0}\right)^{(1/\gamma_b)} - 1} \tag{63}$$

χ is a turbulence augmentation factor, s_{u_o} is the laminar burning velocity, ρ_u is the vapor density of the reactants, G is the unburnt gas mass flux, C_d is the discharge coefficient, A_{st} is the unwetted surface area of the vessel, A_h is the vent area, P_{set} is the set point and P_{max} is the maximum pressure reached during unvented/closed volume combustion.

Solving for the vent area to vessel area ratio leads to the following expression:

$$\frac{A_h}{A_{st}} = \left(\frac{\chi s_{u_o} \rho_u}{G C_d}\right)\left(\frac{\left[\left(\frac{P_f}{P_0}\right)^{(1/\gamma_b)} - \left(\frac{P_{max}}{P_0}\right)^{(1/\gamma_b)}\right]\left[\left(\frac{P_{max}}{P_0}\right)^{(1/\gamma_b)} - 1\right]}{\left(\frac{P_{max}}{P_0}\right)^{(1/\gamma_b)}\left[\left(\frac{P_{set}}{P_0}\right)^{(1/\gamma_b)} - 1\right] - \left(\frac{P_f}{P_0}\right)^{(1/\gamma_b)}\left[\left(\frac{P_{max}}{P_0}\right)^{(1/\gamma_b)}\right] - 1]}\right) \tag{64}$$

The value of G can be estimated using the ideal gas equation for sonic velocity [5]:

$$G = \rho_u \sqrt{\gamma_u \frac{R_g}{M_{w,u}} T_u} \tag{65}$$

where T_u is the absolute temperature of unburnt gases and is estimated using isentropic compression assumptions:

$$T_u = T_0 \left(\frac{P_f}{P_0}\right)^{\frac{\gamma_u - 1}{\gamma_u}} \tag{66}$$

[5] Epstein et al. assumed in their derivation of the above equation (a) ideal gas behavior, (b) uniform temperature in the burnt gas, (c) negligible energy losses to the wall, (d) pressure is uniform throughout the vessel, and (e) when venting occurs only unburned gases are vented.

where T_0 is the initial gas temperature prior to ignition, R_g is the ideal gas constant, 8314 J/kmol/K and $M_{w,u}$ is the average molecular weight of the unburnt gas. Using the above two equations, Equation 64 can be rewritten as follows:

$$\frac{A_h}{A_{st}} = \left(\frac{\chi s_{u_o}}{C_d \sqrt{\gamma_u \frac{R_g}{M_{w,u}} T_u}} \right) \left(\frac{\left[\left(\frac{P_f}{P_0} \right)^{(1/\gamma_b)} - \left(\frac{P_{max}}{P_0} \right)^{(1/\gamma_b)} \right] \left[\left(\frac{P_{max}}{P_0} \right)^{(1/\gamma_b)} - 1 \right]}{\left(\frac{P_{max}}{P_0} \right)^{(1/\gamma_b)} \left[\left(\frac{P_{set}}{P_0} \right)^{(1/\gamma_b)} - 1 \right] - \left(\frac{P_f}{P_0} \right)^{(1/\gamma_b)} \left[\left(\frac{P_{max}}{P_0} \right)^{(1/\gamma_b)} \right] - 1]} \right) \tag{67}$$

Epstein et al. recommend use of the above equation for $Pset/P_0$ values larger than 1.30. The turbulence augmentation factor, χ, represents the ratio of increased burning velocity to the laminar burning velocity. The increase in burning velocity is often due to turbulence generation and the opening of the vent. The sudden opening of a vent (rupture disk, for example) can produce an acoustic wave (pressure) which initiates a hydrodynamic instability within the flame front. Suggested χ values (based on experimental data) for use with the above equation are:

Initially open vent χ ranges from 1 to 2

Initially closed vent χ ranges from 3 to 5

The lower value of χ is recommended if the value of s_{u_o} is less than 0.5 m/s, otherwise the higher χ value should be used. As mentioned earlier in the text, it is possible for deflagrations to run up to detonations if the initial burning velocity is larger than 0.8 m/s and the equipment length to diameter ratio is greater than 5.

C.6 Example: Deflagration Vent Sizing; Vapor/Liquid System

We consider the same 1,000 gallon vessel used in section C.3 which is shown in Figure 23. It is assumed that internal vapor space ignition is the controlling relief scenario. What is the required rupture disk size if the set point is 3 bara ? All data remains the same as in section C.3.

C.6.1 Solution

Equation 67 requires the following data:

1. P_0, pressure prior to ignition; $P_0 = 1$ bara
2. T_0, temperature prior to ignition; $T_0 = 298$ K
3. A_{st}, unwetted internal surface area; $A_{st} = 3.84$ m^2 (see section C.3)
4. χ, turbulence enhancement factor; $\chi = 1.5$
5. s_{u_o}, acetone laminar burning velocity; $s_{u_o} = 0.423$ m/s

6. C_d, discharge coefficient; C_d = 0.6
7. γ_u, acetone ratio of heat capacities; $\gamma_u = 1.103$
8. γ_b, combustion products ratio of heat capacities; $\gamma_b = 1.25$ and $1/\gamma_b = 0.8$
9. M_w, molecular weight of acetone; $M_w = 58.1$
10. P_{max}, maximum pressure reached during unvented combustion. The value of P_{max} can be estimated from the vapor expansion ratio which is calculated in section C.3 to be 9.29. $P_{max} = 9.29$ times the initial pressure or 9.29 bara.
11. P_{set}, set pressure; $P_{set} = 3$ bara.
12. P_f, peak pressure at end of combustion; This value is restricted to 10 % overpressure. $P_f = 1.1 \times 100 + 14.7 = 124.7$ psia or 8.485 bara.
13. T_u, absolute temperature of unburnt gas; T_u is estimated using isentropic compression from equation 66. $T_u = 298 \times (9.29/1)^{(1.103-1)/1.103} = 366.95$ K

The vent area can be estimated using equation 67:

$$\begin{aligned}
\frac{A_h}{A_{st}} &= \left(\frac{1.5 \times 0.423}{0.6\sqrt{1.103 \times (8314/58.1) \times 366.95}}\right)\left(\frac{[8.485^{0.8} - 9.29^{0.8}] \times [9.29^{0.8} - 1]}{9.29^{0.8} \times [3^{0.8} - 1] - 8.485^{0.8} \times [9.29^{0.8} - 1]}\right) \\
&= 0.004394 \times \left(\frac{-2.0589}{8.3769 - 27.378}\right) \\
&= 0.0004761 \\
A_h &= A_{st} \times 0.0004761 = 3.84 \times 0.0004761 = 0.0018283 \text{ m}^2 \\
D_h &= 0.048 \text{ m} \\
&= 1.9 \text{ in}
\end{aligned}$$

The estimated vent diameter is much less than the value obtained in section C.3 of 16.4 inches. In this case, the vessel maximum allowable pressure, P_f, of 8.485 bars is very close to the value of P_{max} of 9.29 bars. A smaller vent diameter of 1.9 inches is required to vent the overpressure due to the low set pressure used. If we raise the set pressure, the required vent diameter will increase as indicated by Equation 67.

Table 13: Typical combustion properties of some hydrocarbons gases and hydrogen in air [37]

Fuel	M_w	LFL V %	UFL V %	C_{stoic} V %	C_{max} V %	s_{u_o} (m/s)	T_f (K)	$\frac{T_f}{288}$	S_f (m/s)	AIT (K)	MIE (mJ)	NCV (MJ/m3)
Hydrogen	2	4	75	30	54	3.50	2,318	8.0	28.0	847	0.02	10.2
Methane	16	5	15	9.5	10	0.45	2,148	7.4	3.50	813	0.29	34
Ethane	30	3	12.5	5.6	6.3	0.53	2,168	7.5	4.0	788	0.24	60.5
Propane	44	2.2	9.5	4.0	4.5	0.52	2,198	7.6	4.0	723	0.25	86.4
Butane	58	1.9	8.5	3.1	3.5	0.50	2,168	7.5	3.7	678	0.25	112.4
Pentane	72	1.5	7.8	2.6	2.9	0.52	2,232	7.7	4.0	533	0.25	138.1
Hexane	86	1.2	7.5	2.2	2.5	0.52	2,221	7.7	4.0	498	0.25	164.4
Heptane	100	1.2	6.7	1.9	2.3	0.52	2,196	7.6	4.0	488	0.25	190.4
Acetylene	26	2.5	80	7.7	9.3	1.58	2,598	9.0	14.2	578	0.02	51
Ethylene	28	3.1	32	6.5	7.4	0.83	2,248	7.8	6.5	763	0.12	56
Propylene	42	2.4	10.3	4.4	5.0	0.66	2,208	7.7	5.1	733	0.28	81.5
Butylene	56	1.7	9.5	3.4	3.9	0.57	2,203	7.6	4.3	658	0.28	107.1
Benzene	78	1.4	7.1	2.7	3.3	0.62	2,287	7.9	4.9	833	0.22	134
Cyclohexane	84	1.3	8.0	2.3	2.7	0.52	2,232	7.8	4.1	518	0.24	167.3
Acetone	58	2.6	12.8							810		
Methanol	32	7.3	36			0.56				737		
Tetrahydrofuran	72.1	2	11.8							594		
Ethyl acetate	88.1	2.2	11.4							700		

1. T_f is the adiabatic flame temperature at 1 bar. Initial temperature of 298 K.
2. $\frac{T_f}{288}$ is the expansion ratio.
3. S_f is the maximum laminar burning velocity estimated from $S_f = s_{u_o} T_f / 288$.
4. AIT is the autoignition temperature.
5. MIE is the minimum ignition energy.
6. NCV is the net calorific (heating) value at 288 K and 1 atm.
7. LFL and UFL are at 1 atm and 298 K.

References

[1] NFPA 68. Standard on explosion protection by deflagration venting, 2018.

[2] G. A. Melhem. A detailed method for the estimation of mixture flammability limits using chemical equilibrium. *Process Safety Progress*, 16(4), 1997.

[3] G. A. Melhem, R. Saini, and B. M. Goodwin. Computation of complex equilibria by direct minimization of the Gibbs free energy. AIChE 1989 Spring National Meeting and Petrochemical Expo, 1989.

[4] G. A. Melhem. Calculate phase and chemical equilibria using Process Safety Office(r) Superchems Expert(tm). *ioMosaic Corporation White Paper*, 2021.

[5] W. Bartknecht. *Explosions*. Springer-Verlag, 1981.

[6] D. Bradley and A. Mitcheson. The venting of gaseous explosions in spherical vessls. i- theory. *Combustion and Flame*, 32:221–236, 1978.

[7] D. Bradley and A. Mitcheson. The venting of gaseous explosions in spherical vessls. ii-theory and experiment. *Combustion and Flame*, 32:237–255, 1978.

[8] R. A. Ogle. *Dust Explosion Dynamics*. Elsevier, 2017.

[9] G. A. Melhem, R. Saini, and B. M. Goodwin. A modified Peng-Robinson equation of state. *Fluid Phase Equilibria*, 47:189–237, 1989.

[10] M. Metghalchi and J. C. Keck. Laminar burning velocity of propane air mixtures at high temperatures and pressure. *Combustion and Flames*, 38:143–154, 1980.

[11] M. Metghalchi and J. C. Keck. *Combustion and Flames*, 48:191–210, 1982.

[12] S. Chippett. Modeling of vented deflagrations. *Combustion and Flame*, 55:127–140, 1984.

[13] D. J. Rasbash, D. D. Drysdale, and N. Kemp. Design of an explosion relief system for a building handling liquefied fuel gases. In *I.Chem. E. Symposium Series No. 49*, 1977.

[14] M. Epstein, I. Swift, and H. Fauske. Estimation of peak pressure for sonic-vented hydrocarbon explosions in spherical vessels. *Combustion and Flame*, 66:1–8, 1986.

[15] A. G. Istratov and V. B. Librovich. On the stability of propagation of spherical flames. *Appl. Mech. Tech. Phys.*, 7:43–50, 1966.

[16] E. Groff. The cellular nature of confined spherical propane-air flames. *Combustion and Flame*, 48:51–62, 1982.

[17] B. E. Milton and J. C. Keck. Laminar burning velocity in stoichiometric hydrogen and hydrocarbon mixtures. *Combustion and Flames*, 58:13–22, 1984.

[18] M. Silvestrini, B. Genova, G. Parisi, and F. J. Leon Trujillo. Flame acceleration and ddt run-up distance for smooth and obstacle filled tubes. *Journal of Loss Prevention in the Process Industries*, 21:555–562, 2008.

[19] C. Proust. Gas flame acceleration in long ducts. `https://hal-ineris.archives-ouvertes.fr/ineris-01862428`, August 2018.

[20] S. B. Dorofeev. Hydrogen flames in tubes: critical run-up distances. *International Journal of Hydrogen Energy*, 34(14):5832–5837, July 2009.

[21] Y. Tanaka. Numerical simulations for combustion of quiescent and turbulent mixtures in confined vessels. *Combustion and Flame*, 75:123–138, 1989.

[22] A. Schack. *Industrial Heat Transfer*. John Wiley & Sons, 1933.

[23] M. Fairweather and M. W. Vasey. A mathematical model for the prediction of overpressures generated in totally confined and vented explosions. In *Nineteenth Symposium on Combustion*, pages 645–653. The Combustion Institute, 1982.

[24] Adam Barowy. Large scale testing of energy storage systems: Fire protection and response considerations, March 6, 2019.

[25] Lars Rogstadkjernet. Combustion of gas in closed, interconnected vessels: Pressure piling. Master's thesis, University of Bergen, 2004.

[26] Rolf Eckhoff. *Dust Explosions in the Process Industries*. Gulf Professional Publishing, 3rd edition, 2003.

[27] G. A. Melhem. Get the most out of your deflagration test data - dusts, gases, and hybrid systems. In *DIERS Users Group Meeting*. AIChE, Spring 2007.

[28] Gibbs and Calcote. *Journal of Chem. Eng. Data*, 4:226, 1959.

[29] Laurence G. Britton. Static hazards using flexible intermediate bulk containers for powder handling. *Process Safety Progress*, 12(4), 1993.

[30] B. Lewis and G. von Elbe. *Combustion, Flames and Explosions of Gases*. Academic Press, 3rd edition, 1987.

[31] C. J. Dahn, B. N. Reyes, and A. Kashani. Electrostatic discharge (ESD) energy initiation of dust cloud. In *Powder and Bulk Solids Conference*, pages 1–11, 1991.

[32] M. G. Zabetakis. *Flammability Characteristics of Combustible Gases and Vapors. Bulletin 627*. Bureau of Mines, 1965.

[33] Guide for venting of deflagrations. National Fire Protection Association (NFPA), 1988.

[34] I. Swift and M. Epstein. Performance of low pressure explosion vents. *Plant and Operations Progress*, 6(2), 1987.

[35] K. N. Palmer. *Dust Explosions and Fires*. Chapman and Hall, 1973.

[36] Pressure release of dust explosion. VDI Richtilinie 3673, Verein Deustscher Ingenieure - Kommision Reinhaltung der Luft, Dusseldorf, 1979-1983.

[37] R. J. Harris. *The Investigation and Control of Gas Explosions In Buildings and Heating Plant*. British Gas, 1983.

Index

About the Author

Dr. Melhem is an internationally known pressure relief and flare systems, chemical reaction systems, process safety, and risk analysis expert. In this regard he has provided consulting, design services, expert testimony, incident investigation, and incident reconstruction for a large number of clients. Since 1988, he has conducted and participated in numerous studies focused on the risks associated with process industries fixed facilities, facility siting, business interruption, and transportation.

Prior to founding ioMosaic Corporation, Dr. Melhem was president of Pyxsys Corporation; a technology subsidiary of Arthur D. Little Inc. Prior to Pyxsys and during his twelve years tenure at Arthur D. Little, Dr. Melhem was a vice president of Arthur D. Little and managing director of its Global Safety and Risk Management Practice and Process Safety and Reaction Engineering Laboratories.

Dr. Melhem holds a Ph.D. and an M.S. in Chemical Engineering, as well as a B.S. in Chemical Engineering with a minor in Industrial Engineering, all from Northeastern University. In addition, he has completed executive training in the areas of Finance and Strategic Sales Management at the Harvard Business School. Dr. Melhem is a Fellow of the American Institute of Chemical Engineers (AIChE) and Vice Chair of the AIChE Design Institute for Emergency Relief Systems (DiERS).

Contact Information

Georges. A. Melhem, Ph.D., FAIChE
E-mail. melhem@iomosaic.com

ioMosaic Corporation
93 Stiles Road
Salem, New Hampshire 03079
Tel. 603.893.7009, x 1001
Fax. 603.251.8384
web. www.iomosaic.com

How can we help?

In addition to our deep experience in process safety management (PSM) and the conduct of large-scale site wide relief systems evaluations by both static and dynamic methods, we understand the many non-technical and subtle aspects of regulatory compliance and legal requirements. When you work with ioMosaic you have a trusted ISO certified partner that you can rely on for assistance and support with the lifecycle costs of relief systems to achieve optimal risk reduction and PSM compliance that you can evergreen. We invite you to connect the dots with ioMosaic.

We also offer laboratory testing services through ioKinetic for the characterization of chemical reactivity and dust/flammability hazards. ioKinetic is an ISO accredited, ultra-modern testing facility that can assist in minimizing operational risks. Our experienced professionals will help you define what you need, conduct the testing, interpret the data, and conduct detailed analysis. All with the goal of helping you identify your hazards, define and control your risk.

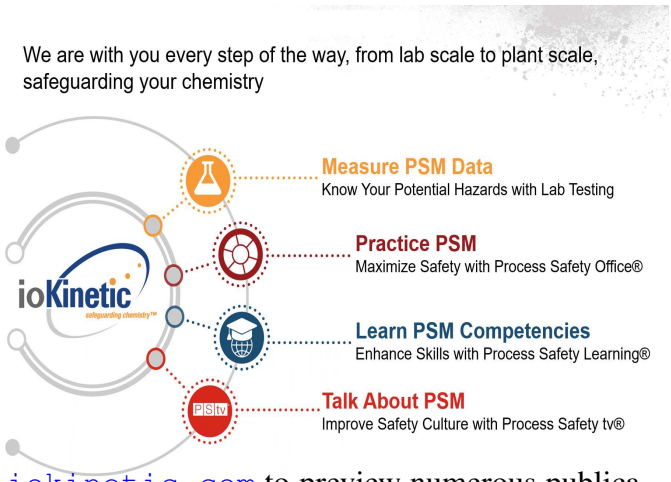

Please visit www.iomosaic.com and www.iokinetic.com to preview numerous publications on process safety management, chemical reactivity and dust hazards characterization, safety moments, video papers, software solutions, and online training.

ioMosaic®

Minimizing risk. Maximizing potential.®

US Offices

New Hampshire (Salem) – *Headquarters*
Texas (Houston)
Minnesota (Minneapolis)
California (Berkeley)

International Offices

Kingdom of Bahrain (Al Seef)
United Kingdom (Bath)

Software Solutions

Process Safety Enterprise®
Centralize the process safety management lifecycle to accelerate business goals

Process Safety Office®
Identify, evaluate, and control process hazards with tools used by process safety consultants

Process Safety Learning®
Build your process safety competencies incrementally with online training

Process Safety tv®
View, share, and discuss PSM worldwide on a secure platform

Contact Us

www.ioMosaic.com
sales@ioMosaic.com
1.844.ioMosaic

About ioMosaic Corporation

Through innovation and dedication to continual improvement, ioMosaic has become a leading provider of integrated process safety and risk management solutions. ioMosaic has expertise in a wide variety of areas, including pressure relief systems design, process safety management, expert litigation support, laboratory services, training and software development.

As a certified ISO 9001:2015 Quality Management System (QMS) company, ioMosaic offers integrated process safety and risk management services to help you manage and reduce episodic risk. Because when safety, efficiency, and compliance are improved, you can sleep better at night. Our extensive expertise allows us the flexibility, resources, and capabilities to determine what you need to reduce and manage episodic risk, maintain compliance, and prevent injuries and catastrophic incidents.

Our mission is to help you protect your people, plant, stakeholder value, and our planet.

Consulting Services

- Asset Integrity
- Auditing and Due Diligence
- Combustible Dust Hazard Analysis and Testing
- Facility Siting
- Fault Tree/SIL/SIS Analysis
- Fire and Explosion Dynamics
- Incident Investigation, Litigation Support and Expert Testimony
- Liquefied Natural Gas Safety
- Pipeline Safety
- Process Engineering Design and Support
- Process Hazards Analysis (PHA)
- Process Safety Management (PSM)
- Reactive Chemicals Evaluation and Testing
- Relief and Flare Systems Design and Evaluations
- Risk Management Program Development
- Quantitative Risk Assessments (QRA)
- Software Solutions
- Structural Dynamics
- Training

Laboratory Testing Services (ISO accredited)

- Chemical Reactivity
- Combustible Dust
- Battery Safety
- Specialized Testing